containing either only one maternal allele or two alleles. Imprinting usually blocks IGF-2 expression from the maternal allele in liver. However, IGF-2 re-expression occurred in all 4 of these models, and was chronologically associated with late stages of progression toward HCC [113].

Epidermal growth factor (EGF) is a potent mitogen to hepatocytes. Unlike in other malignancies, the EGF receptor is rarely mutated in HCC, and several reports suggest an EGF-mediated autocrine growth stimulation of hepatoma cells [114]. This was further supported by the accelerated liver tumor formation after constitutive over-expression of a secretable form of EGF (IgEGF). All double-transgenic mice with liver-specific IgEGF over-expression in cooperation with AAT-myc died by 4.4 months from HCC, whereas only 44% of ATT-myc mice had developed HCC by age 14 months [115].

3.3.3.5. Wnt/β-catenin pathway. A key pathway implicated in hepatic tumorigenesis is the canonical Wnt pathway, in which β-catenin acts as a co-activator of the TCF/LEF family of transcription factors and regulates the expression of several genes related to cell proliferation and apoptosis. The Wnt/β-catenin signaling pathway normally functions in cellular differentiation, proliferation, and apoptosis, and has a fundamental role in embryogenesis. Liver development in xenopus, zebrafish, and mouse embryogenesis has been shown to be dependent on functional Wnt signaling [116,117].

There is general agreement that Wnt signaling is upregulated in a subset of HCCs [118]. Mutations of genes encoding several components of the Wnt pathway have been described, including β-catenin (19–44%), AXIN1 and AXIN2 (5–14% and 3–10%) [119–123]. The mutations of β-catenin identified in HCC are located in exon 3 of the CTNNB1 gene, the phosphorylation site for GSK3α/β. In addition, immunohistological studies have demonstrated abnormal cytoplasmic and nuclear accumulation of β-catenin in 17–40% of human HCCs [124,125]. In addition to accumulated mutations, stimulation of proliferation in liver cancer cell lines transfected with Hepatitis C core viral protein is at least partially mediated by upregulation of Wnt-1 protein expression [126]. This correlation between HCV and the Wnt pathway needs to be verified by *in vivo* studies.

Although mutations in β-catenin are thought to be tumorigenic in human HCCs, transgenic mouse models over-expressing either a stable mutant form of β-catenin [127,128] or a constitutively activated, non-mutated form of β-catenin exhibit hepatomegaly, but no HCC [127–129]. Surprisingly, although mutations in the tumor suppressor APC are very rarely seen in HCC and patients with germline APC mutations do not typically develop HCC, it has been found that liver-targeted loss of APC in mice can lead to HCC through activation of β-catenin signaling [130].

It seems that a second hit from an additional mutation is required to generate tumors in β-catenin transgenic mice. Simultaneous co-expression of a Wnt-activating β-catenin mutation ($Catnb^{lox(ex3)}$) and mutation in H-ras introduced by adenovirus-mediated Cre expression resulted in HCC in 100% of the double-transgenic progeny [131]. The interplay between the growth factor signaling pathways and the Wnt/β-catenin pathway was amply illustrated in the simultaneous over-expression of HGF and β-catenin knockout mouse model generated by Monga and colleagues [96]: the proliferative effects of HGF over-expression were mediated by β-catenin stabilization, and were negated in β-catenin null mice.

3.3.4. Other HCC models

3.3.4.1. Fibroblast growth factor in muscle. While most mouse models of HCC express growth factors and oncogenes under liver-specific promoters, liver-specific expression is not a requirement for development of HCC. For example, a transgenic model over-expressing fibroblast growth factor 19 (FGF19) in skeletal muscle develops HCC in 53% of mice by age 10–12 months [132]. Interestingly, unlike the vast majority of both human tumors and murine models, these tumors are more common in female progeny. Hepatocellular proliferation was significantly increased in these mice and in non-transgenic mice injected with FGF19 protein. Furthermore, immunostaining for β-catenin revealed nuclear staining in 4/4 female mouse tumors, and subsequent sequencing of the GSK3β phosphorylation site of β-catenin revealed mutations in 16%, which implicates activation of the Wnt/β-catenin signaling pathway as a potential mechanism for hepatocellular transformation in this model.

3.3.4.2. Urokinase-type plasminogen activator. Not all genetically modified models of HCC arise from predicted oncogene over-expression, tumor suppressor loss, or liver injury. In a transgenic model over-expressing the urokinase-type plasminogen activator (*uPA*) transgene under the albumin promoter, for example, most mice died from liver hemorrhage within 4 days of birth; in the two transgenic lineages developed from surviving founder mice, there was a surprising 100% incidence of HCC at 8–20 months of age. Moreover, the surviving mice regained normal clotting function, and their livers were repopulated by clonal, regenerative nodules that no longer expressed the transgene. Tumor progenitor cells were found to contain transgene-deleting chromosomal rearrangements which likely extended into flanking DNA. Therefore, the initiating event in this HCC model was likely extensive DNA rearrangements occurring during rapid regeneration [133].

3.4. Chemically-induced fibrosis and hepatocarcinogenesis

Cirrhosis is a major cause of mortality as both a precursor to malignancy and a cause for liver failure. As a disease with clear environmental non-hereditary components to its aetiology, liver fibrosis and cancer is well suited for modeling using chemical induction. Experimental models of liver disease can be categorized as cholestatic, nutritional, alcoholic, immunological, and toxic, and have been reviewed elsewhere [134].

Briefly, several hepatotoxic agents have been used both in the induction of generalized liver disease and HCC (see Table 3). Chemical models of hepatocarcinogenesis often involve initiation by a carcinogen followed by a growth stimulus promoter to induce clonal expansion of initiated cells, such as partial hepatectomy (Solt–Farber method [135]) or phenobarbital [136]. Alternatively, rodents are subjected to repeated administration of carcinogens such as DEN, DMN, or CCl_4 over a prolonged period [136]. Most initiated cells accrue damage and ultimately undergo apoptosis, but the small number that respond to promoters evolve into dysplastic foci and later to dysplastic nodules. These foci and nodules can disappear following the removal of promoters in a process termed remodeling, which typically involves apoptosis of the preneoplastic cells [41]. Nodules which have acquired the capacity for autonomous growth progress to neoplastic nodules and HCC, an irreversible process involving the accumulation of genomic damage [137].

The most commonly employed model for liver disease is carbon tetrachloride (CCl_4) administered in drinking water, in inhaled gases, or by intraperitoneal injection. The reactive metabolite trichloromethyl radical is produced during the oxidative metabolism of CCl_4 by cytochrome p450, and causes liver damage by eliciting production of reactive oxygen intermediates and by peroxidative degradation of membrane phospholipids [138]. Compounds like phenobarbital, ethanol, and acetone induce microsomal cytochrome p450 and therefore potentiate the hepatotoxicity of CCl_4, as does hypoxia; therefore, hepatocellular injury and necrosis are predominantly seen in the centrolobular zone where the oxygen tension is low [134,138].

Dimethylnitrosamine (DMN) is a carcinogenic agent which causes liver injury by covalent binding and methylation of nucleic acids and proteins in hepatocytes [139]. Animals administered DMN either per oral or by intraperitoneal injection develop cirrhosis within 3–4 weeks, and can continue to have stable or progressive disease for several months after discontinuation of the agent [140].

Diethylnitrosamine (DEN) induces pericentral foci of small dysplastic hepatocytes and acts by ethylating nucleophilic sites in DNA [141,142], causing cirrhosis and multifocal HCC within 18 weeks [89,143]. Frequent β-catenin mutations have been found in HCCs induced by DENA in mice [144], and when combined with a methyl-deficient diet, DEN administration generates p53 mutation or rearrangement in rats [145].

Thioacetamide (TAA) in drinking water (0.03%) or by intraperitoneal injection induces fibrosis in rats and mice over a period of 2–3 months, which may be secondary to the oxidant properties of TAA and the induction of hepatic oxidative stress [134,146,147]. Acute liver injury and subsequent fibrosis can be created by administration of D-galactosamine (GalN), a hepatotoxin that induces liver damage by depleting uridine nucleotides and therefore diminishing RNA and protein synthesis [148].

Cholestatic cirrhosis has been induced by extrahepatic bile duct ligation (BDL) in rats, rabbits, dogs, and monkeys. Histologically, the BDL model is characterized by infiltration of connective tissue in the portal

Table 3
Toxic models of liver fibrosis and HCC

Diet or chemical	Mechanism of action	Phenotype	References
Choline-deficient and ethionine (CDE) diet	Oxidative DNA damage, DNA strand breaks and chromosomal instability [41]	30–35 weeks: 100% HCC	[135,190–192]
Ciprofibrate	Synthetic peroxisome proliferators, non-genotoxic carcinogen	60 weeks: 100% HCC [193]	[90,193,194]
Diethylnitrosamine (DENA)	Genotoxic hepatocarcinogen	100% HCC in males, 30% in females. Extensive chromosomal damage	[90,168,194,195]
Thioacetamide (TAA)	Metabolites induce oxidative stress	100% HCC	[134,146]
2-Acetylaminoflouren (2-AAF)	Genotoxic	Used primarily as promoter in initiation/promotion protocols	[194,196]
Phenobarbital	Non-genotoxic	Used as promoter in initiation/promotion protocols; increases HCC by 500%. Can inhibit tumor formation in mice given DEN. Associated with β-catenin activation [197]	[197,198]

zone and proliferation of bile duct epithelial cells and hepatocytes. This methods allows rapid four-week induction of cirrhosis, and the mortality is high [134].

Choline-, methionine-deficient diets administered over 3–12 week periods induce cirrhosis and HCC in rats and mice, even when followed by an adequate diet [41]. Injury in these diets is most likely attributable to depletion of hepatic antioxidant mechanisms, such as reduced glutathione, which leads to oxidative DNA damage, inflammation and fibrosis [41,149]. Histologic changes seen in rodents fed this diet include periportal fatty liver, focal hepatocyte necrosis, oval cell proliferation, infrequent cirrhosis [150] and HCC [151]. The variation in animal susceptibility to choline deficiency is a disadvantage to this model [134].

3.5. Models of liver fibrosis and HCC: creating a tumor environment

The tumor microenvironment is emerging as a fundamental determinant of oncogenesis and metastasis. The liver presents an ideal organ in which to study the interaction between tumors and their microenvironment, as hepatocellular carcinoma (HCC) develops in a background of liver fibrosis in about 90% of cases. While the notion that the tumor microenvironment may help instigate tumor formation is gaining acceptance, the manner in which this occurs remains a mystery. In addition to the traditional toxic method of inducing fibrosis in rodents, there are numerous transgenic models that have been designed to recapitulate the phenotype of chronic inflammation leading to fibrosis and HCC seen in humans (see Table 4).

Stellate cell transactivation is a hallmark of hepatic fibrogenesis. Many genetic models of liver fibrosis have focused on the over-expression of TGF-β, a major fibrogenic factor that drives matrix deposition from activated stellate cells [152]. Sanderson et al. generated transgenic mice containing a fusion gene (Alb/TGF-β1) under the control of the regulatory elements of the mouse albumin gene; these mice developed mild fibrosis by 12 weeks, and rarely developed cirrhosis [153]. Similar mild to moderately fibrotic phenotypes have been demonstrated by other investigators [154,155]. When exposed to thioacetamide, TGF-β1-over-expressing transgenic mice develop fibrosis at an accelerated rate [155], and develop HCC more frequently than wild-type mice (9/9 versus 4/10 mice at 9 months) [156].

Intracellular signaling from TGF-β occurs through signaling members TGF-β receptor type II (TBRII), SMAD2, SMAD4, and SMAD adaptor, which are tumor suppressors in gastrointestinal cancers. None of

Table 4
Genetically modified models of liver fibrosis, inflammation, and HCC

Gene	Type of mutation or tissue promotor/construct	Phenotype	Dysplasia or HCC	References
TGF-β	Porcine TGF-β over-expression under albumin promoter	Early death due to extra-intestinal manifestations [153]; mild fibrosis [155,156]	100% HCC in transgenic mice treated with TAA [156]	[153,155,156]
TGF-β inducible transgenic	Fusion CRP/TGF-β1 under CRP promotor, induced by LPS injection	Collagen deposition at age 6 weeks	None reported	[154]
$ELF^{+/-}$ knockout	ELF+/− knockout mice	Steatosis	40% HCC at >15 months	[157,199]
PDGF-B	PDGF-B over-expression using Cre-LoxP under albumin promoter; made Tamoxifene-inducible by breeding with mice expressing Cre under transthyretin receptor promoter	100% liver fibrosis at age 4–6 weeks	None reported	[159]
PDGF-C	Human PDGF-C expression driven by albumin promoter	Fibrosis and steatosis	80% HCC at 12 months	[160]
IL-6 knockout	IL-6 knockout ($IL\text{-}6^{-/-}$)	Hepatocyte necrosis and compensatory proliferation both decreased in $IL\text{-}6^{-/-}$ mice	<10% HCC in $IL\text{-}6^{-/-}$ mice compared to 100% HCC at 8 months in male WT mice; 13% HCC in female WT mice	[162,163]
MyD88 knockout	$MyD88^{-/-}$	Diminished production of IL-6 in $MyD88^{-/-}$ mice	Suppression of DEN-induced HCC: $MyD88^{-/-}$ mice had fewer smaller HCCs than WT mice	[162,163]
Alpha-1-antitrypsin (AAT)	Transgenic mice using AAT Z genomic clones	High copy Z lineage: AAT accumulation in endoplasmic reticulum; hepatitis and HCC	82% HCC at 16-18 months	[164]
Mdr-2	Mdr-2 gene knockout	Early: non-suppurative inflammatory cholangitis	HCC at 6–12 months with +lung metastasis [166]	[165,166]
$Acox1^{-/-}$	Fatty acyl-CoA oxidase null ($AOX^{-/-}$) [167]	Steatohepatitis followed by regeneration	100% HCC at 15 months [167]	[167]

the SMAD mutant models have developed HCC, however. SMAD function is dependent upon adaptor proteins such as embryonic liver fodrin (ELF), a β-spectrin protein. ELF associates with SMAD3, SMAD 4, and the TGF-β receptor complex, and ultimately leads to their translocation to the nucleus. Mishra et al. report that $ELF^{+/-}$ knockout mice develop steatosis and spontaneous HCC. Loss of ELF in these mice results in cell cycle disruption with significant increases in Cdk4, cyclin D1 and pRb hyperphosphorylation [157].

In addition to TGF-β, activated stellate cells produce a number of other profibrotic cytokines such as platelet derived growth factor (PDGF). Induction of PDGF receptor mRNA is one of the earliest events in stellate cell activation, and its over-expression has been linked to fibrosis [158]. Kanzler's group developed a model in which the PDGF-B ligand is inducibly over-expressed in the liver. They found that PDGF-B expression caused hepatic stellate cell activation and collagen deposition [159]. Campbell et al. have described a PDGF-C transgenic model expressing human PDGF-C driven by the albumin promoter. These mice develop fibrosis and steatosis, and 80% develop HCC by 12 months of age [160]. Interestingly, no cirrhosis or regenerating nodules were observed in either of these models.

Interleukin-6 (IL-6) is the cytokine largely responsible for hepatic response to infections and inflammation. IL-6 serum concentrations are increased in patients with HBV and HCV infections and with HCC [161]. Naugler et al. induced liver disease with DEN in IL-6 knockout ($IL\text{-}6^{-/-}$) mice to determine whether gender bias in IL-6 production accounts for the sex difference seen in HCC development in both humans and in rodent models [162]. The carcinogenic effects of DEN were suppressed in $IL\text{-}6^{-/-}$ male mice: <10% developed HCC by 8 months of age, compared to 100% in wild-type male mice. No difference was seen in $IL\text{-}6^{-/-}$ versus WT female mice. Estrogens inhibit IL-6 promoter activity by decreasing activity of the transcription factors NF-κB and C/EBPβ, a process dependent on IKKβ and toll-like receptor (TLR) adaptor Myd-88. In the same study, Myd-88 was found to be required for IL-6 induction by necrotic hepatocyte debris, and Myd-88 knockout ($Myd\text{-}88^{-/-}$) male mice developed fewer and smaller HCCs in response to injury by DEN than did WT male mice. The results of this experiment provide a potential explanation for the gender differences in the incidence of liver cancer, which ranges between 2:1 and 4:1 male to female ratio [163].

Alpha-1-antitrypsin (AAT)-deficient transgenic mice express the transport-impaired Z variant of the human disease. These mice accumulate AAT and form foci of hyperplasia surrounded by inflammatory infiltrates [41], developing hepatitis, adenomas after 12 months, and HCC after 16–20 months [164].

The Mdr-2 gene encodes a protein involved in transport of phosphatidylcholine into the bile. Mdr-2 knockout mice accumulate toxic bile salts in their intrahepatic biliary system, which causes a non-suppurative inflammatory cholangitis and ductular proliferation and eventually nodules and HCC at 6–12 months [165,166]. A similar pathogenesis occurs in acyl-CoA oxidase (AOX) knockout mice, which develop steatohepatitis followed by a complete liver regeneration; this sequence of inflammation followed by proliferation results in the formation of HCCs by the age of 15 months [167].

4. Integrating functional genomics in HCC: from mice to humans

The progression from dysplastic foci to HCC involves the accumulation of genetic changes which can be monitored with cytogenetic studies that show karyotypic alterations in various chromosomes [137]. This type of chromosomal gains and losses are particularly numerous in lesions from rodents subjected to the carcinogen initiator–promoter protocol, or in SV40/T antigen transgenic mice. Various genes involved in hepatocarcinogenesis such as c-H-ras, met, HGF, myc, and p53 are located on rat chromosomes exhibiting frequent aberrations [41].

Thorgeirrson et al. applied a genome-wide microarray analysis to three transgenic mouse models of HCC, and found that although gene expression profiles in tumors derived from the three transgenic lines were highly similar, it was possible to identify oncogene-specific gene expression signatures at an early dysplastic stage of hepatocarcinogenesis [168]. In a related study, gene expression patterns of HCC tumors from seven different mouse models and 91 human HCCs from predefined subclasses were measured to compare the molecular features of mouse and human HCCs [90]. The authors found that gene expression patterns in tumors from Myc, E2f1 and Myc/E2f1 transgenic mice were similar to those of the better survival group of human HCC, whereas the expression patterns in HCCs from Myc/Tgfα transgenic mice and from DEN-treated mice were most similar to those of the poorer survival group of human HCC. Gene expression patterns in HCC from $Acox1^{-/-}$ mice and in ciprofibrate-induced HCCs were least similar to those observed in human HCCs. This study supports the notion that comparison of gene expression between the two species can be used to identify the mouse models of HCC that most closely mimic the tumors in humans.

5. Conclusion

We have described both traditional models of carcinogenesis in which the expression of oncogenes and tumor suppressor genes is genetically altered to produce

HCC, and other models in which tumor formation is dependent on inflammation. The natural history of HCC development in humans, combined with the evidence that genetic mutations alone sometimes do not generate tumors unless initiated by a proinflammatory agent, underscore the need to develop new models in which HCCs develop spontaneously in an environment of fibrosis, in order to best recapitulate the human disease process. In addition, integrative functional genomic studies have suggested that human HCCs can be classified into subgroups based on molecular pathway activation. Comparison of gene expression between mouse models and human HCC may allow us to create mouse models in future which recapitulate the various subgroups, which would make ideal models for preclinical studies.

Acknowledgement

We dedicate this work to our friend and colleague Eric Lemmer, M.D., Ph.D., whose presence at its inception was highly inspirational, and whose absence today we still lament.

References

[1] El-Serag HB, Rudolph KL. Hepatocellular carcinoma: epidemiology and molecular carcinogenesis. Gastroenterology 2007;132:2557–2576.
[2] Farazi PA, DePinho RA. Hepatocellular carcinoma pathogenesis: from genes to environment. Nat Rev Cancer 2006;6:674–687.
[3] Chiang D. Focal VEGFA gains and molecular classification of hepatocellular carcinomas. Hepatology 2007;46:530A.
[4] Frese KK, Tuveson DA. Maximizing mouse cancer models. Nat Rev Cancer 2007;7:654–658.
[5] Rygaard J, Povlsen CO. Heterotransplantation of a human malignant tumour to "Nude" mice. Acta Pathol Microbiol Scand 1969;77:758–760.
[6] Kelland LR. Of mice and men: values and liabilities of the athymic nude mouse model in anticancer drug development. Eur J Cancer 2004;40:827–836.
[7] Venditti JM. Preclinical drug development: rationale and methods. Semin Oncol 1981;8:349–361.
[8] Alley MC, Scudiero DA, Monks A, Hursey ML, Czerwinski MJ, Fine DL, et al. Feasibility of drug screening with panels of human tumor cell lines using a microculture tetrazolium assay. Cancer Res 1988;48:589–601.
[9] Monks A, Scudiero D, Skehan P, Shoemaker R, Paull K, Vistica D, et al. Feasibility of a high-flux anticancer drug screen using a diverse panel of cultured human tumor cell lines. J Natl Cancer Inst 1991;83:757–766.
[10] Johnson JI, Decker S, Zaharevitz D, Rubinstein LV, Venditti JM, Schepartz S, et al. Relationships between drug activity in NCI preclinical *in vitro* and *in vivo* models and early clinical trials. Br J Cancer 2001;84:1424–1431.
[11] Voskoglou-Nomikos T, Pater JL, Seymour L. Clinical predictive value of the *in vitro* cell line, human xenograft, and mouse allograft preclinical cancer models. Clin Cancer Res 2003;9:4227–4239.
[12] Kerbel RS. Human tumor xenografts as predictive preclinical models for anticancer drug activity in humans: better than commonly perceived-but they can be improved. Cancer Biol Ther 2003;2:S134–S139.
[13] Inaba M, Kobayashi T, Tashiro T, Sakurai Y. Pharmacokinetic approach to rational therapeutic doses for human tumor-bearing nude mice. Jpn J Cancer Res 1988;79:509–516.
[14] De Both NJ, Vermey M, Groen N, Dinjens WN, Bosman FT. Clonal growth of colorectal-carcinoma cell lines transplanted to nude mice. Int J Cancer 1997;72:1137–1141.
[15] Staroselsky AN, Radinsky R, Fidler IJ, Pathak S, Chernajovsky Y, Frost P. The use of molecular genetic markers to demonstrate the effect of organ environment on clonal dominance in a human renal-cell carcinoma grown in nude mice. Int J Cancer 1992;51:130–138.
[16] Hoffman RM. Orthotopic metastatic (MetaMouse) models for discovery and development of novel chemotherapy. Methods Mol Med 2005;111:297–322.
[17] Karnoub AE, Dash AB, Vo AP, Sullivan A, Brooks MW, Bell GW, et al. Mesenchymal stem cells within tumour stroma promote breast cancer metastasis. Nature 2007;449:557–563.
[18] Wu C, Wei Q, Utomo V, Nadesan P, Whetstone H, Kandel R, et al. Side population cells isolated from mesenchymal neoplasms have tumor initiating potential. Cancer Res 2007;67:8216–8222.
[19] Tuveson DA, Jacks T. Technologically advanced cancer modeling in mice. Curr Opin Genet Dev 2002;12:105–110.
[20] Rangarajan A, Weinberg RA. Opinion: comparative biology of mouse versus human cells: modelling human cancer in mice. Nat Rev Cancer 2003;3:952–959.
[21] Blasco MA, Lee HW, Hande MP, Samper E, Lansdorp PM, DePinho RA, et al. Telomere shortening and tumor formation by mouse cells lacking telomerase RNA. Cell 1997;91:25–34.
[22] Maddison K, Clarke AR. New approaches for modelling cancer mechanisms in the mouse. J Pathol 2005;205:181–193.
[23] Jaenisch R. Transgenic animals. Science 1988;240:1468–1474.
[24] Macleod KF, Jacks T. Insights into cancer from transgenic mouse models. J Pathol 1999;187:43–60.
[25] Jacks T, Fazeli A, Schmitt EM, Bronson RT, Goodell MA, Weinberg RA. Effects of an Rb mutation in the mouse. Nature 1992;359:295–300.
[26] Robanus-Maandag E, Dekker M, van der Valk M, Carrozza ML, Jeanny JC, Dannenberg JH, et al. p107 is a suppressor of retinoblastoma development in pRb-deficient mice. Genes Dev 1998;12:1599–1609.
[27] Adams JM, Harris AW, Pinkert CA, Corcoran LM, Alexander WS, Cory S, et al. The c-myc oncogene driven by immunoglobulin enhancers induces lymphoid malignancy in transgenic mice. Nature 1985;318:533–538.
[28] Gannon M, Gamer LW, Wright CV. Regulatory regions driving developmental and tissue-specific expression of the essential pancreatic gene pdx1. Dev Biol 2001;238:185–201.
[29] Mattick JS, Makunin IV. Non-coding RNA. Hum Mol Genet 2006;15:R17–R29.
[30] Palmiter RD, Brinster RL. Germ-line transformation of mice. Annu Rev Genet 1986;20:465–499.
[31] Dorer DR. Do transgene arrays form heterochromatin in vertebrates? Transgenic Res 1997;6:3–10.
[32] Politi K, Kljuic A, Szabolcs M, Fisher P, Ludwig T, Efstratiadis A. 'Designer' tumors in mice. Oncogene 2004;23:1558–1565.
[33] Jonkers J, Berns A. Conditional mouse models of sporadic cancer. Nat Rev Cancer 2002;2:251–265.
[34] Baron U, Bujard H. Tet repressor-based system for regulated gene expression in eukaryotic cells: principles and advances. Methods Enzymol 2000;327:401–421.
[35] Gossen M, Freundlieb S, Bender G, Muller G, Hillen W, Bujard H. Transcriptional activation by tetracyclines in mammalian cells. Science 1995;268:1766–1769.
[36] Le Y, Sauer B. Conditional gene knockout using Cre recombinase. Mol Biotechnol 2001;17:269–275.

[37] Branda CS, Dymecki SM. Talking about a revolution: The impact of site-specific recombinases on genetic analyses in mice. Dev Cell 2004;6:7–28.
[38] Sadowski PD. The Flp recombinase of the 2-microns plasmid of *Saccharomyces cerevisiae*. Prog Nucleic Acid Res Mol Biol 1995;51:53–91.
[39] Lakso M, Sauer B, Mosinger Jr B, Lee EJ, Manning RW, Yu SH, et al. Targeted oncogene activation by site-specific recombination in transgenic mice. Proc Natl Acad Sci USA 1992;89:6232–6236.
[40] Feo F, De Miglio MR, Simile MM, Muroni MR, Calvisi DF, Frau M, et al. Hepatocellular carcinoma as a complex polygenic disease. Interpretive analysis of recent developments on genetic predisposition. Biochim Biophys Acta 2006;1765:126–147.
[41] Feo F, Pascale R, Calvisi D. Models for liver cancer. In: Alison M, editor. The cancer handbook. John Wiley & Sons; 2007, 1–16.
[42] Huynh H, Soo KC, Chow PK, Panasci L, Tran E. Xenografts of human hepatocellular carcinoma: a useful model for testing drugs. Clin Cancer Res 2006;12:4306–4314.
[43] Ma S, Chan KW, Hu L, Lee TK, Wo JY, Ng IO, et al. Identification and characterization of tumorigenic liver cancer stem/progenitor cells. Gastroenterology 2007;132:2542–2556.
[44] Ma S, Lee TK, Zheng BJ, Chan KW, Guan XY. CD133(+) HCC cancer stem cells confer chemoresistance by preferential expression of the Akt/PKB survival pathway. Oncogene 2008;27:1749–1758.
[45] Kornek M, Raskopf E, Tolba R, Becker U, Klockner M, Sauerbruch T, et al. Accelerated orthotopic HCC growth is linked to increased expression of pro-angiogenic and pro-metastatic factors in murine liver fibrosis. Liver Int 2008;28:509–518.
[46] Rustgi VK. The epidemiology of hepatitis C infection in the United States. J Gastroenterol 2007;42:513–521.
[47] Chisari FV, Klopchin K, Moriyama T, Pasquinelli C, Dunsford HA, Sell S, et al. Molecular pathogenesis of hepatocellular carcinoma in hepatitis B virus transgenic mice. Cell 1989;59:1145–1156.
[48] Koike K, Moriya K, Iino S, Yotsuyanagi H, Endo Y, Miyamura T, et al. High-level expression of hepatitis B virus HBx gene and hepatocarcinogenesis in transgenic mice. Hepatology 1994;19:810–819.
[49] Yu DY, Moon HB, Son JK, Jeong S, Yu SL, Yoon H, et al. Incidence of hepatocellular carcinoma in transgenic mice expressing the hepatitis B virus X-protein. J Hepatol 1999;31:123–132.
[50] Slagle BL, Lee TH, Medina D, Finegold MJ, Butel JS. Increased sensitivity to the hepatocarcinogen diethylnitrosamine in transgenic mice carrying the hepatitis B virus X gene. Mol Carcinog 1996;15:261–269.
[51] Koike K. Transgenic mouse models of viral hepatitis: insight into viral hepatocarcinogenesis. Viral Hepatitis Rev 1999;5:177–203.
[52] Chisari FV, Filippi P, Buras J, McLachlan A, Popper H, Pinkert CA, et al. Structural and pathological effects of synthesis of hepatitis B virus large envelope polypeptide in transgenic mice. Proc Natl Acad Sci USA 1987;84:6909–6913.
[53] Dunsford HA, Sell S, Chisari FV. Hepatocarcinogenesis due to chronic liver cell injury in hepatitis B virus transgenic mice. Cancer Res 1990;50:3400–3407.
[54] Liang TJ, Heller T. Pathogenesis of hepatitis C-associated hepatocellular carcinoma. Gastroenterology 2004;127:S62–S71.
[55] Kawamura T, Furusaka A, Koziel MJ, Chung RT, Wang TC, Schmidt EV, et al. Transgenic expression of hepatitis C virus structural proteins in the mouse. Hepatology 1997;25:1014–1021.
[56] Kamegaya Y, Hiasa Y, Zukerberg L, Fowler N, Blackard JT, Lin W, et al. Hepatitis C virus acts as a tumor accelerator by blocking apoptosis in a mouse model of hepatocarcinogenesis. Hepatology 2005;41:660–667.
[57] Moriya K, Yotsuyanagi H, Shintani Y, Fujie H, Ishibashi K, Matsuura Y, et al. Hepatitis C virus core protein induces hepatic steatosis in transgenic mice. J Gen Virol 1997;78:1527–1531.
[58] Moriya K, Fujie H, Shintani Y, Yotsuyanagi H, Tsutsumi T, Ishibashi K, et al. The core protein of hepatitis C virus induces hepatocellular carcinoma in transgenic mice. Nat Med 1998;4:1065–1067.
[59] Koike K, Moriya K, Kimura S. Role of hepatitis C virus in the development of hepatocellular carcinoma: transgenic approach to viral hepatocarcinogenesis. J Gastroenterol Hepatol 2002;17:394–400.
[60] Lerat H, Honda M, Beard MR, Loesch K, Sun J, Yang Y, et al. Steatosis and liver cancer in transgenic mice expressing the structural and nonstructural proteins of hepatitis C virus. Gastroenterology 2002;122:352–365.
[61] Moriya K, Todoroki T, Tsutsumi T, Fujie H, Shintani Y, Miyoshi H, et al. Increase in the concentration of carbon 18 monounsaturated fatty acids in the liver with hepatitis C: analysis in transgenic mice and humans. Biochem Biophys Res Commun 2001;281:1207–1212.
[62] Moriya K, Nakagawa K, Santa T, Shintani Y, Fujie H, Miyoshi H, et al. Oxidative stress in the absence of inflammation in a mouse model for hepatitis C virus-associated hepatocarcinogenesis. Cancer Res 2001;61:4365–4370.
[63] Radaeva S, Li Y, Hacker HJ, Burger V, Kopp-Schneider A, Bannasch P. Hepadnaviral hepatocarcinogenesis: in situ visualization of viral antigens, cytoplasmic compartmentation, enzymic patterns, and cellular proliferation in preneoplastic hepatocellular lineages in woodchucks. J Hepatol 2000;33:580–600.
[64] Tennant BC, Toshkov IA, Peek SF, Jacob JR, Menne S, Hornbuckle WE, et al. Hepatocellular carcinoma in the woodchuck model of hepatitis B virus infection. Gastroenterology 2004;127:S283–S293.
[65] Yang D, Alt E, Rogler CE. Coordinate expression of N-myc 2 and insulin-like growth factor II in precancerous altered hepatic foci in woodchuck hepatitis virus carriers. Cancer Res 1993;53:2020–2027.
[66] Farazi PA, Glickman J, Horner J, Depinho RA. Cooperative interactions of p53 mutation, telomere dysfunction, and chronic liver damage in hepatocellular carcinoma progression. Cancer Res 2006;66:4766–4773.
[67] Lewis BC, Klimstra DS, Socci ND, Xu S, Koutcher JA, Varmus HE. The absence of p53 promotes metastasis in a novel somatic mouse model for hepatocellular carcinoma. Mol Cell Biol 2005;25:1228–1237.
[68] Chen YW, Klimstra DS, Mongeau ME, Tatem JL, Boyartchuk V, Lewis BC. Loss of p53 and Ink4a/Arf cooperate in a cell autonomous fashion to induce metastasis of hepatocellular carcinoma cells. Cancer Res 2007;67:7589–7596.
[69] Xue W, Zender L, Miething C, Dickins RA, Hernando E, Krizhanovsky V, et al. Senescence and tumour clearance is triggered by p53 restoration in murine liver carcinomas. Nature 2007;445:656–660.
[70] Yamasaki L. Balancing proliferation and apoptosis *in vivo*: the Goldilocks theory of E2F/DP action. Biochim Biophys Acta 1999;1423:M9–M15.
[71] Conner EA, Lemmer ER, Omori M, Wirth PJ, Factor VM, Thorgeirsson SS. Dual functions of E2F-1 in a transgenic mouse model of liver carcinogenesis. Oncogene 2000;19:5054–5062.
[72] Calvisi DF, Conner EA, Ladu S, Lemmer ER, Factor VM, Thorgeirsson SS. Activation of the canonical Wnt/beta-catenin pathway confers growth advantages in c-myc/E2F1 transgenic mouse model of liver cancer. J Hepatol 2005;42:842–849.
[73] Ali SH, DeCaprio JA. Cellular transformation by SV40 large T antigen: interaction with host proteins. Semin Cancer Biol 2001;11:15–23.
[74] Sandgren EP, Quaife CJ, Pinkert CA, Palmiter RD, Brinster RL. Oncogene-induced liver neoplasia in transgenic mice. Oncogene 1989;4:715–724.

[75] Manickan E, Satoi J, Wang TC, Liang TJ. Conditional liver-specific expression of simian virus 40 T antigen leads to regulatable development of hepatic neoplasm in transgenic mice. J Biol Chem 2001;276:13989–13994.
[76] Hayflick L, Moorhead PS. The serial cultivation of human diploid cell strains. Exp Cell Res 1961;25:585–621.
[77] Artandi SE, DePinho RA. Mice without telomerase: what can they teach us about human cancer? Nat Med 2000;6: 852–855.
[78] Hastie ND, Dempster M, Dunlop MG, Thompson AM, Green DK, Allshire RC. Telomere reduction in human colorectal carcinoma and with ageing. Nature 1990;346:866–868.
[79] Llovet JM, Chen Y, Wurmbach E, Roayaie S, Fiel MI, Schwartz M, et al. A molecular signature to discriminate dysplastic nodules from early hepatocellular carcinoma in HCV cirrhosis. Gastroenterology 2006;131:1758–1767.
[80] Satra M, Gatselis N, Iliopoulos D, Zacharoulis D, Dalekos GN, Tsezou A. Real-time quantification of human telomerase reverse transcriptase mRNA in liver tissues from patients with hepatocellular cancer and chronic viral hepatitis. J Viral Hepat 2007;14:41–47.
[81] Miura N, Horikawa I, Nishimoto A, Ohmura H, Ito H, Hirohashi S, et al. Progressive telomere shortening and telomerase reactivation during hepatocellular carcinogenesis. Cancer Genet Cytogenet 1997;93:56–62.
[82] Wiemann SU, Satyanarayana A, Tsahuridu M, Tillmann HL, Zender L, Klempnauer J, et al. Hepatocyte telomere shortening and senescence are general markers of human liver cirrhosis. Faseb J 2002;16:935–942.
[83] Plentz RR, Caselitz M, Bleck JS, Gebel M, Flemming P, Kubicka S, et al. Hepatocellular telomere shortening correlates with chromosomal instability and the development of human hepatoma. Hepatology 2004;40:80–86.
[84] Kipling D, Cooke HJ. Hypervariable ultra-long telomeres in mice. Nature 1990;347:400–402.
[85] Artandi SE, Chang S, Lee SL, Alson S, Gottlieb GJ, Chin L, et al. Telomere dysfunction promotes non-reciprocal translocations and epithelial cancers in mice. Nature 2000;406:641–645.
[86] Jhappan C, Stahle C, Harkins RN, Fausto N, Smith GH, Merlino GT. TGF alpha overexpression in transgenic mice induces liver neoplasia and abnormal development of the mammary gland and pancreas. Cell 1990;61:1137–1146.
[87] Lee GH, Merlino G, Fausto N. Development of liver tumors in transforming growth factor alpha transgenic mice. Cancer Res 1992;52:5162–5170.
[88] Sandgren EP, Luetteke NC, Palmiter RD, Brinster RL, Lee DC. Overexpression of TGF alpha in transgenic mice: induction of epithelial hyperplasia, pancreatic metaplasia, and carcinoma of the breast. Cell 1990;61:1121–1135.
[89] Schiffer E, Housset C, Cacheux W, Wendum D, Desbois-Mouthon C, Rey C, et al. Gefitinib, an EGFR inhibitor, prevents hepatocellular carcinoma development in the rat liver with cirrhosis. Hepatology 2005;41:307–314.
[90] Lee JS, Chu IS, Mikaelyan A, Calvisi DF, Heo J, Reddy JK, et al. Application of comparative functional genomics to identify best-fit mouse models to study human cancer. Nat Genet 2004;36:1306–1311.
[91] Wang R, Ferrell LD, Faouzi S, Maher JJ, Bishop JM. Activation of the Met receptor by cell attachment induces and sustains hepatocellular carcinomas in transgenic mice. J Cell Biol 2001;153:1023–1034.
[92] Zender L, Spector MS, Xue W, Flemming P, Cordon-Cardo C, Silke J, et al. Identification and validation of oncogenes in liver cancer using an integrative oncogenomic approach. Cell 2006;125:1253–1267.
[93] Park WS, Dong SM, Kim SY, Na EY, Shin MS, Pi JH, et al. Somatic mutations in the kinase domain of the Met/hepatocyte growth factor receptor gene in childhood hepatocellular carcinomas. Cancer Res 1999;59:307–310.
[94] Takami T, Kaposi-Novak P, Uchida K, Gomez-Quiroz LE, Conner EA, Factor VM, et al. Loss of hepatocyte growth factor/c-Met signaling pathway accelerates early stages of *N*-nitrosodiethylamine induced hepatocarcinogenesis. Cancer Res 2007;67:9844–9851.
[95] Sakata H, Takayama H, Sharp R, Rubin JS, Merlino G, LaRochelle WJ. Hepatocyte growth factor/scatter factor overexpression induces growth, abnormal development, and tumor formation in transgenic mouse livers. Cell Growth Differ 1996;7:1513–1523.
[96] Apte U, Zeng G, Muller P, Tan X, Micsenyi A, Cieply B, et al. Activation of Wnt/beta-catenin pathway during hepatocyte growth factor-induced hepatomegaly in mice. Hepatology 2006;44:992–1002.
[97] Santoni-Rugiu E, Preisegger KH, Kiss A, Audolfsson T, Shiota G, Schmidt EV, et al. Inhibition of neoplastic development in the liver by hepatocyte growth factor in a transgenic mouse model. Proc Natl Acad Sci USA 1996;93:9577–9582.
[98] Shiota G, Kawasaki H, Nakamura T, Schmidt EV. Characterization of double transgenic mice expressing hepatocye growth factor and transforming growth factor alpha. Res Commun Mol Pathol Pharmacol 1995;90:17–24.
[99] Tward AD, Jones KD, Yant S, Cheung ST, Fan ST, Chen X, et al. Distinct pathways of genomic progression to benign and malignant tumors of the liver. Proc Natl Acad Sci USA 2007;104:14771–14776.
[100] Bellacosa A, Testa JR, Staal SP, Tsichlis PN. A retroviral oncogene, akt, encoding a serine-threonine kinase containing an SH2-like region. Science 1991;254:274–277.
[101] Staal SP, Hartley JW, Rowe WP. Isolation of transforming murine leukemia viruses from mice with a high incidence of spontaneous lymphoma. Proc Natl Acad Sci USA 1977;74:3065–3067.
[102] Bellacosa A, de Feo D, Godwin AK, Bell DW, Cheng JQ, Altomare DA, et al. Molecular alterations of the AKT2 oncogene in ovarian and breast carcinomas. Int J Cancer 1995;64:280–285.
[103] Vivanco I, Sawyers CL. The phosphatidylinositol 3-Kinase AKT pathway in human cancer. Nat Rev Cancer 2002;2:489–501.
[104] Stanger BZ, Stiles B, Lauwers GY, Bardeesy N, Mendoza M, Wang Y, et al. Pten constrains centroacinar cell expansion and malignant transformation in the pancreas. Cancer Cell 2005;8:185–195.
[105] Bernal-Mizrachi E, Wen W, Stahlhut S, Welling CM, Permutt MA. Islet beta cell expression of constitutively active Akt1/PKB alpha induces striking hypertrophy, hyperplasia, and hyperinsulinemia. J Clin Invest 2001;108:1631–1638.
[106] Shioi T, McMullen JR, Kang PM, Douglas PS, Obata T, Franke TF, et al. Akt/protein kinase B promotes organ growth in transgenic mice. Mol Cell Biol 2002;22:2799–2809.
[107] Majumder PK, Febbo PG, Bikoff R, Berger R, Xue Q, McMahon LM, et al. mTOR inhibition reverses Akt-dependent prostate intraepithelial neoplasia through regulation of apoptotic and HIF-1-dependent pathways. Nat Med 2004;10:594–601.
[108] Horie Y, Suzuki A, Kataoka E, Sasaki T, Hamada K, Sasaki J, et al. Hepatocyte-specific Pten deficiency results in steatohepatitis and hepatocellular carcinomas. J Clin Invest 2004;113:1774–1783.
[109] Watanabe S, Horie Y, Kataoka E, Sato W, Dohmen T, Ohshima S, et al. Non-alcoholic steatohepatitis and hepatocellular carcinoma: lessons from hepatocyte-specific phosphatase and tensin homolog (PTEN)-deficient mice. J Gastroenterol Hepatol 2007;22:S96–S100.
[110] Breuhahn K, Longerich T, Schirmacher P. Dysregulation of growth factor signaling in human hepatocellular carcinoma. Oncogene 2006;25:3787–3800.

[111] Braulke T. Type-2 IGF receptor: a multi-ligand binding protein. Horm Metab Res 1999;31:242–246.
[112] Iizuka N, Oka M, Yamada-Okabe H, Mori N, Tamesa T, Okada T, et al. Comparison of gene expression profiles between hepatitis B virus- and hepatitis C virus-infected hepatocellular carcinoma by oligonucleotide microarray data on the basis of a supervised learning method. Cancer Res 2002;62:3939–3944.
[113] Schirmacher P, Held WA, Yang D, Chisari FV, Rustum Y, Rogler CE. Reactivation of insulin-like growth factor II during hepatocarcinogenesis in transgenic mice suggests a role in malignant growth. Cancer Res 1992;52:2549–2556.
[114] Yamaguchi K, Carr BI, Nalesnik MA. Concomitant and isolated expression of TGF-alpha and EGF-R in human hepatoma cells supports the hypothesis of autocrine, paracrine, and endocrine growth of human hepatoma. J Surg Oncol 1995;58:240–245.
[115] Tonjes RR, Lohler J, O'Sullivan JF, Kay GF, Schmidt GH, Dalemans W, et al. Autocrine mitogen IgEGF cooperates with c-myc or with the Hcs locus during hepatocarcinogenesis in transgenic mice. Oncogene 1995;10:765–768.
[116] Tan X, Behari J, Cieply B, Michalopoulos GK, Monga SP. Conditional deletion of beta-catenin reveals its role in liver growth and regeneration. Gastroenterology 2006;131:1561–1572.
[117] McLin VA, Zorn AM. Molecular control of liver development. Clin Liver Dis 2006;10:1–25.
[118] Thorgeirsson SS, Grisham JW. Molecular pathogenesis of human hepatocellular carcinoma. Nat Genet 2002;31:339–346.
[119] Satoh S, Daigo Y, Furukawa Y, Kato T, Miwa N, Nishiwaki T, et al. AXIN1 mutations in hepatocellular carcinomas, and growth suppression in cancer cells by virus-mediated transfer of AXIN1. Nat Genet 2000;24:245–250.
[120] Miyoshi Y, Iwao K, Nagasawa Y, Aihara T, Sasaki Y, Imaoka S, et al. Activation of the beta-catenin gene in primary hepatocellular carcinomas by somatic alterations involving exon 3. Cancer Res 1998;58:2524–2527.
[121] de La Coste A, Romagnolo B, Billuart P, Renard CA, Buendia MA, Soubrane O, et al. Somatic mutations of the beta-catenin gene are frequent in mouse and human hepatocellular carcinomas. Proc Natl Acad Sci USA 1998;95:8847–8851.
[122] Taniguchi K, Roberts LR, Aderca IN, Dong X, Qian C, Murphy LM, et al. Mutational spectrum of beta-catenin, AXIN1, and AXIN2 in hepatocellular carcinomas and hepatoblastomas. Oncogene 2002;21:4863–4871.
[123] Laurent-Puig P, Legoix P, Bluteau O, Belghiti J, Franco D, Binot F, et al. Genetic alterations associated with hepatocellular carcinomas define distinct pathways of hepatocarcinogenesis. Gastroenterology 2001;120:1763–1773.
[124] Wong CM, Fan ST, Ng IO. beta-Catenin mutation and overexpression in hepatocellular carcinoma: clinicopathologic and prognostic significance. Cancer 2001;92:136–145.
[125] Wei Y, Van Nhieu JT, Prigent S, Srivatanakul P, Tiollais P, Buendia MA. Altered expression of E-cadherin in hepatocellular carcinoma: correlations with genetic alterations, beta-catenin expression, and clinical features. Hepatology 2002;36:692–701.
[126] Fukutomi T, Zhou Y, Kawai S, Eguchi H, Wands JR, Li J. Hepatitis C virus core protein stimulates hepatocyte growth: correlation with upregulation of wnt-1 expression. Hepatology 2005;41:1096–1105.
[127] Cadoret A, Ovejero C, Saadi-Kheddouci S, Souil E, Fabre M, Romagnolo B, et al. Hepatomegaly in transgenic mice expressing an oncogenic form of beta-catenin. Cancer Res 2001;61:3245–3249.
[128] Harada N, Miyoshi H, Murai N, Oshima H, Tamai Y, Oshima M, et al. Lack of tumorigenesis in the mouse liver after adenovirus-mediated expression of a dominant stable mutant of beta-catenin. Cancer Res 2002;62:1971–1977.
[129] Tan X, Apte U, Micsenyi A, Kotsagrelos E, Luo JH, Ranganathan S, et al. Epidermal growth factor receptor: a novel target of the Wnt/beta-catenin pathway in liver. Gastroenterology 2005;129:285–302.
[130] Colnot S, Decaens T, Niwa-Kawakita M, Godard C, Hamard G, Kahn A, et al. Liver-targeted disruption of Apc in mice activates beta-catenin signaling and leads to hepatocellular carcinomas. Proc Natl Acad Sci USA 2004;101:17216–17221.
[131] Harada N, Oshima H, Katoh M, Tamai Y, Oshima M, Taketo MM. Hepatocarcinogenesis in mice with beta-catenin and Ha-ras gene mutations. Cancer Res 2004;64:48–54.
[132] Nicholes K, Guillet S, Tomlinson E, Hillan K, Wright B, Frantz GD, et al. A mouse model of hepatocellular carcinoma: ectopic expression of fibroblast growth factor 19 in skeletal muscle of transgenic mice. Am J Pathol 2002;160:2295–2307.
[133] Sandgren EP, Palmiter RD, Heckel JL, Brinster RL, Degen JL. DNA rearrangement causes hepatocarcinogenesis in albumin–plasminogen activator transgenic mice. Proc Natl Acad Sci USA 1992;89:11523–11527.
[134] Claria J, Jimenez W. Experimental models of cirrhosis and ascites. In: Gines PAV, Rodes J, Schrier RW, editors. Ascites and Renal Dysfunction in Liver Disease: Pathogenesis, Diagnosis, and Treatment. Malden, Massachusetts: Blackwell Publishing; 2005. p. 215–226.
[135] Solt DB, Medline A, Farber E. Rapid emergence of carcinogen-induced hyperplastic lesions in a new model for the sequential analysis of liver carcinogenesis. Am J Pathol 1977;88:595–618.
[136] Farber E, Sarma DS. Hepatocarcinogenesis: a dynamic cellular perspective. Lab Invest 1987;56:4–22.
[137] Feo F, Pascale RM, Simile MM, De Miglio MR, Muroni MR, Calvisi D. Genetic alterations in liver carcinogenesis: implications for new preventive and therapeutic strategies. Crit Rev Oncog 2000;11:19–62.
[138] McCay PB, Lai EK, Poyer JL, DuBose CM, Janzen EG. Oxygen- and carbon-centered free radical formation during carbon tetrachloride metabolism. Observation of lipid radicals *in vivo* and *in vitro*. J Biol Chem 1984;259:2135–2143.
[139] Encell L, Foiles PG, Gold B. The relationship between *N*-nitrosodimethylamine metabolism and DNA methylation in isolated rat hepatocytes. Carcinogenesis 1996;17:1127–1134.
[140] Jenkins SA, Grandison A, Baxter JN, Day DW, Taylor I, Shields R. A dimethylnitrosamine-induced model of cirrhosis and portal hypertension in the rat. J Hepatol 1985;1:489–499.
[141] Goldfarb S, Pugh TD, Koen H, He YZ. Preneoplastic and neoplastic progression during hepatocarcinogenesis in mice injected with diethylnitrosamine in infancy. Environ Health Perspect 1983;50:149–161.
[142] Koen H, Pugh TD, Goldfarb S. Centrilobular distribution of diethylnitrosamine-induced hepatocellular foci in the mouse. Lab Invest 1983;49:78–81.
[143] Pascale RM, Simile MM, Feo F. Genomic abnormalities in hepatocarcinogenesis. Implications for a chemopreventive strategy. Anticancer Res 1993;13:1341–1356.
[144] Tsujiuchi T, Tsutsumi M, Sasaki Y, Takahama M, Konishi Y. Different frequencies and patterns of beta-catenin mutations in hepatocellular carcinomas induced by *N*-nitrosodiethylamine and a choline-deficient L-amino acid-defined diet in rats. Cancer Res 1999;59:3904–3907.
[145] Gomez-Angelats M, Teeguarden JG, Dragan YP, Pitot HC. Mutational analysis of three tumor suppressor genes in two models of rat hepatocarcinogenesis. Mol Carcinog 1999;25:157–163.
[146] Li X, Benjamin IS, Alexander B. Reproducible production of thioacetamide-induced macronodular cirrhosis in the rat with no mortality. J Hepatol 2002;36:488–493.
[147] Kang JS, Morimura K, Salim EI, Wanibuchi H, Yamaguchi S, Fukushima S. Persistence of liver cirrhosis in association with proliferation of nonparenchymal cells and altered location of

alpha-smooth muscle actin-positive cells. Toxicol Pathol 2005;33:329–335.
[148] Keppler DO, Pausch J, Decker K. Selective uridine triphosphate deficiency induced by D-galactosamine in liver and reversed by pyrimidine nucleotide precursors. Effect on ribonucleic acid synthesis. J Biol Chem 1974;249:211–216.
[149] Ghoshal AK, Ahluwalia M, Farber E. The rapid induction of liver cell death in rats fed a choline-deficient methionine-low diet. Am J Pathol 1983;113:309–314.
[150] Rushmore TH, Ghazarian DM, Subrahmanyan V, Farber E, Ghoshal AK. Probable free radical effects on rat liver nuclei during early hepatocarcinogenesis with a choline-devoid low methionine diet. Cancer Res 1987;47:6731–6740.
[151] Chandar N, Lombardi B. Liver cell proliferation and incidence of hepatocellular carcinomas in rats fed consecutively a choline-devoid and a choline-supplemented diet. Carcinogenesis 1988;9:259–263.
[152] Bissell DM, Wang SS, Jarnagin WR, Roll FJ. Cell-specific expression of transforming growth factor-beta in rat liver. Evidence for autocrine regulation of hepatocyte proliferation. J Clin Invest 1995;96:447–455.
[153] Sanderson N, Factor V, Nagy P, Kopp J, Kondaiah P, Wakefield L, et al. Hepatic expression of mature transforming growth factor beta 1 in transgenic mice results in multiple tissue lesions. Proc Natl Acad Sci USA 1995;92:2572–2576.
[154] Kanzler S, Lohse AW, Keil A, Henninger J, Dienes HP, Schirmacher P, et al. TGF-beta1 in liver fibrosis: an inducible transgenic mouse model to study liver fibrogenesis. Am J Physiol 1999;276:G1059–G1068.
[155] Schnur J, Olah J, Szepesi A, Nagy P, Thorgeirsson SS. Thioacetamide-induced hepatic fibrosis in transforming growth factor beta-1 transgenic mice. Eur J Gastroenterol Hepatol 2004;16:127–133.
[156] Schnur J, Nagy P, Sebestyen A, Schaff Z, Thorgeirsson SS. Chemical hepatocarcinogenesis in transgenic mice overexpressing mature TGF beta-1 in liver. Eur J Cancer 1999;35:1842–1845.
[157] Kitisin K, Ganesan N, Tang Y, Jogunoori W, Volpe EA, Kim SS, et al. Disruption of transforming growth factor-beta signaling through beta-spectrin ELF leads to hepatocellular cancer through cyclin D1 activation. Oncogene 2007;26:7103–7110.
[158] Wong L, Yamasaki G, Johnson RJ, Friedman SL. Induction of beta-platelet-derived growth factor receptor in rat hepatic lipocytes during cellular activation *in vivo* and in culture. J Clin Invest 1994;94:1563–1569.
[159] Czochra P, Klopcic B, Meyer E, Herkel J, Garcia-Lazaro JF, Thieringer F, et al. Liver fibrosis induced by hepatic overexpression of PDGF-B in transgenic mice. J Hepatol 2006;45:419–428.
[160] Campbell JS, Hughes SD, Gilbertson DG, Palmer TE, Holdren MS, Haran AC, et al. Platelet-derived growth factor C induces liver fibrosis, steatosis, and hepatocellular carcinoma. Proc Natl Acad Sci USA 2005;102:3389–3394.
[161] Abiru S, Migita K, Maeda Y, Daikoku M, Ito M, Ohata K, et al. Serum cytokine and soluble cytokine receptor levels in patients with non-alcoholic steatohepatitis. Liver Int 2006;26:39–45.
[162] Naugler WE, Sakurai T, Kim S, Maeda S, Kim K, Elsharkawy AM, et al. Gender disparity in liver cancer due to sex differences in MyD88-dependent IL-6 production. Science 2007;317:121–124.
[163] Wands J. Hepatocellular carcinoma and sex. N Engl J Med 2007;357:1974–1976.
[164] Geller SA, Nichols WS, Kim S, Tolmachoff T, Lee S, Dycaico MJ, et al. Hepatocarcinogenesis is the sequel to hepatitis in Z#2 alpha 1-antitrypsin transgenic mice: histopathological and DNA ploidy studies. Hepatology 1994;19:389–397.
[165] Katzenellenbogen M, Pappo O, Barash H, Klopstock N, Mizrahi L, Olam D, et al. Multiple adaptive mechanisms to chronic liver disease revealed at early stages of liver carcinogenesis in the Mdr2-knockout mice. Cancer Res 2006;66:4001–4010.
[166] Mauad TH, van Nieuwkerk CM, Dingemans KP, Smit JJ, Schinkel AH, Notenboom RG, et al. Mice with homozygous disruption of the mdr2 P-glycoprotein gene. A novel animal model for studies of nonsuppurative inflammatory cholangitis and hepatocarcinogenesis. Am J Pathol 1994;145:1237–1245.
[167] Fan CY, Pan J, Usuda N, Yeldandi AV, Rao MS, Reddy JK. Steatohepatitis, spontaneous peroxisome proliferation and liver tumors in mice lacking peroxisomal fatty acyl-CoA oxidase. Implications for peroxisome proliferator-activated receptor alpha natural ligand metabolism. J Biol Chem 1998;273:15639–15645.
[168] Coulouarn C, Gomez-Quiroz LE, Lee JS, Kaposi-Novak P, Conner EA, Goldina TA, et al. Oncogene-specific gene expression signatures at preneoplastic stages in mice define distinct mechanisms of hepatocarcinogenesis. Hepatology 2006;44: 1003–1011.
[169] Guerra C, Schuhmacher AJ, Canamero M, Grippo PJ, Verdaguer L, Perez-Gallego L, et al. Chronic pancreatitis is essential for induction of pancreatic ductal adenocarcinoma by K-Ras oncogenes in adult mice. Cancer Cell 2007;11:291–302.
[170] Hingorani SR, Wang L, Multani AS, Combs C, Deramaudt TB, Hruban RH, et al. Trp53R172H and KrasG12D cooperate to promote chromosomal instability and widely metastatic pancreatic ductal adenocarcinoma in mice. Cancer Cell 2005;7:469–483.
[171] Santoni-Rugiu E, Jensen MR, Thorgeirsson SS. Disruption of the pRb/E2F pathway and inhibition of apoptosis are major oncogenic events in liver constitutively expressing c-myc and transforming growth factor alpha. Cancer Res 1998;58: 123–134.
[172] Chien WM, Garrison K, Caufield E, Orthel J, Dill J, Fero ML. Differential gene expression of p27Kip1 and Rb knockout pituitary tumors associated with altered growth and angiogenesis. Cell Cycle 2007;6:750–757.
[173] Wong AK, Chin L. An inducible melanoma model implicates a role for RAS in tumor maintenance and angiogenesis. Cancer Metastasis Rev 2000;19:121–129.
[174] Wu X, Wu J, Huang J, Powell WC, Zhang J, Matusik RJ, et al. Generation of a prostate epithelial cell-specific Cre transgenic mouse model for tissue-specific gene ablation. Mech Dev 2001;101:61–69.
[175] Chisari FV, Pinkert CA, Milich DR, Filippi P, McLachlan A, Palmiter RD, et al. A transgenic mouse model of the chronic hepatitis B surface antigen carrier state. Science 1985;230:1157–1160.
[176] Toshkov I, Chisari FV, Bannasch P. Hepatic preneoplasia in hepatitis B virus transgenic mice. Hepatology 1994;20: 1162–1172.
[177] Jacks T, Remington L, Williams BO, Schmitt EM, Halachmi S, Bronson RT, et al. Tumor spectrum analysis in p53-mutant mice. Curr Biol 1994;4:1–7.
[178] Santoni-Rugiu E, Nagy P, Jensen MR, Factor VM, Thorgeirsson SS. Evolution of neoplastic development in the liver of transgenic mice co-expressing c-myc and transforming growth factor-alpha. Am J Pathol 1996;149:407–428.
[179] Conner EA, Lemmer ER, Sanchez A, Factor VM, Thorgeirsson SS. E2F1 blocks and c-myc accelerates hepatic ploidy in transgenic mouse models. Biochem Biophys Res Commun 2003;302:114–120.
[180] Dalemans W, Perraud F, Le Meur M, Gerlinger P, Courtney M, Pavirani A. Heterologous protein expression by transimmortalized differentiated liver cell lines derived from transgenic mice (hepatomas/alpha 1 antitrypsin/ONC mouse). Biologicals 1990;18:191–198.
[181] Perraud F, Dalemans W, Gendrault JL, Dreyer D, Ali-Hadji D, Faure T, et al. Characterization of trans-immortalized hepatic cell lines established from transgenic mice. Exp Cell Res 1991;195:59–65.

[182] Murakami H, Sanderson ND, Nagy P, Marino PA, Merlino G, Thorgeirsson SS. Transgenic mouse model for synergistic effects of nuclear oncogenes and growth factors in tumorigenesis: interaction of c-myc and transforming growth factor alpha in hepatic oncogenesis. Cancer Res 1993;53:1719–1723.
[183] Schirmacher P, Held WA, Yang D, Biempica L, Rogler CE. Selective amplification of periportal transitional cells precedes formation of hepatocellular carcinoma in SV40 large tag transgenic mice. Am J Pathol 1991;139:231–241.
[184] Messing A, Chen HY, Palmiter RD, Brinster RL. Peripheral neuropathies, hepatocellular carcinomas and islet cell adenomas in transgenic mice. Nature 1985;316:461–463.
[185] Sepulveda AR, Finegold MJ, Smith B, Slagle BL, DeMayo JL, Shen RF, et al. Development of a transgenic mouse system for the analysis of stages in liver carcinogenesis using tissue-specific expression of SV40 large T-antigen controlled by regulatory elements of the human alpha-1-antitrypsin gene. Cancer Res 1989;49:6108–6117.
[186] Dubois N, Bennoun M, Allemand I, Molina T, Grimber G, Daudet-Monsac M, et al. Time-course development of differentiated hepatocarcinoma and lung metastasis in transgenic mice. J Hepatol 1991;13:227–239.
[187] Rogler CE, Yang D, Rossetti L, Donohoe J, Alt E, Chang CJ, et al. Altered body composition and increased frequency of diverse malignancies in insulin-like growth factor-II transgenic mice. J Biol Chem 1994;269:13779–13784.
[188] Harris TM, Rogler LE, Rogler CE. Reactivation of the maternally imprinted IGF2 allele in TGFalpha induced hepatocellular carcinomas in mice. Oncogene 1998;16:203–209.
[189] Shiota G, Wang TC, Nakamura T, Schmidt EV. Hepatocyte growth factor in transgenic mice: effects on hepatocyte growth, liver regeneration and gene expression. Hepatology 1994;19:962–972.
[190] Yaswen P, Goyette M, Shank PR, Fausto N. Expression of c-Ki-ras, c-Ha-ras, and c-myc in specific cell types during hepatocarcinogenesis. Mol Cell Biol 1985;5:780–786.
[191] Chandar N, Lombardi B, Locker J. c-myc gene amplification during hepatocarcinogenesis by a choline-devoid diet. Proc Natl Acad Sci USA 1989;86:2703–2707.
[192] Nagy P, Evarts RP, Marsden E, Roach J, Thorgeirsson SS. Cellular distribution of c-myc transcripts during chemical hepatocarcinogenesis in rats. Cancer Res 1988;48:5522–5527.
[193] Rao MS, Lalwani ND, Watanabe TK, Reddy JK. Inhibitory effect of antioxidants ethoxyquin and 2(3)-tert-butyl-4-hydroxyanisole on hepatic tumorigenesis in rats fed ciprofibrate, a peroxisome proliferator. Cancer Res 1984;44:1072–1076.
[194] Groos J, Bannasch P, Schwarz M, Kopp-Schneider A. Comparison of mode of action of four hepatocarcinogens: a model-based approach. Toxicol Sci 2007;99:446–454.
[195] Poirier LA. Hepatocarcinogenesis by diethylnitrosamine in rats fed high dietary levels of lipotropes. J Natl Cancer Inst 1975;54:137–140.
[196] Williams GM, Iatropoulos MJ, Wang CX, Jeffrey AM, Thompson S, Pittman B, et al. Nonlinearities in 2-acetylaminofluorene exposure responses for genotoxic and epigenetic effects leading to initiation of carcinogenesis in rat liver. Toxicol Sci 1998;45:152–161.
[197] Calvisi DF, Ladu S, Factor VM, Thorgeirsson SS. Activation of beta-catenin provides proliferative and invasive advantages in c-myc/TGF-alpha hepatocarcinogenesis promoted by phenobarbital. Carcinogenesis 2004;25:901–908.
[198] Lee GH. Paradoxical effects of phenobarbital on mouse hepatocarcinogenesis. Toxicol Pathol 2000;28:215–225.
[199] Tang Y, Katuri V, Dillner A, Mishra B, Deng CX, Mishra L. Disruption of transforming growth factor-beta signaling in ELF beta-spectrin-deficient mice. Science 2003;299:574–577.

Int. J. Cancer: **122**, 124–131 (2008)

Hepatitis C virus core protein induces spontaneous and persistent activation of peroxisome proliferator-activated receptor α in transgenic mice: Implications for HCV-associated hepatocarcinogenesis

Naoki Tanaka[1,2]*, Kyoji Moriya[3], Kendo Kiyosawa[2], Kazuhiko Koike[3] and Toshifumi Aoyama[1]

[1]*Department of Metabolic Regulation, Institute on Aging and Adaptation, Shinshu University Graduate School of Medicine, Matsumoto, Japan*

[2]*Division of Gastroenterology, Department of Internal Medicine, Shinshu University School of Medicine, Matsumoto, Japan*

[3]*Department of Internal Medicine, Graduate School of Medicine, University of Tokyo, Tokyo, Japan*

Persistent infection of hepatitis C virus (HCV) can lead to a high risk for hepatocellular carcinoma (HCC). HCV core protein plays important roles in HCV-related hepatocarcinogenesis, because mice carrying the core protein exhibit multicentric HCCs without hepatic inflammation and fibrosis. However, the precise mechanism of hepatocarcinogenesis in these transgenic mice remains unclear. To evaluate whether the core protein modulates hepatocyte proliferation and apoptosis *in vivo*, we examined these parameters in 9- and 22-month-old transgenic mice. Although the numbers of apoptotic hepatocytes and hepatic caspase 3 activities were similar between transgenic and nontransgenic mice, the numbers of proliferating hepatocytes and the levels of numerous proteins such as cyclin D1, cyclin-dependent kinase 4 and c-Myc, were markedly increased in an age-dependent manner in the transgenic mice. This increase was correlated with the activation of peroxisome proliferator-activated receptor α (PPARα). In these transgenic mice, spontaneous and persistent PPARα activation occurred heterogeneously, which was different from that observed in mice treated with clofibrate, a potent peroxisome proliferator. We further demonstrated that stabilization of PPARα through a possible interaction with HCV core protein and an increase in nonesterified fatty acids, which may serve as endogenous PPARα ligands, in hepatocyte nuclei contributed to the core protein-specific PPARα activation. In conclusion, these results offer the first suggestion that HCV core protein induces spontaneous, persistent, age-dependent and heterogeneous activation of PPARα in transgenic mice, which may contribute to the age-dependent and multicentric hepatocarcinogenesis mediated by the core protein.

Key words: cell-cycle regulator; peroxisome; nuclear stabilization; heterogeneous PPARα activation

Hepatitis C virus (HCV) is one of the major causes of chronic hepatitis, and persistent infection with this virus can lead to a high incidence of hepatocellular carcinoma (HCC).[1,2] The prevalence of HCC because of chronic HCV infection has increased over the past two decades,[3,4] and chronic HCV infection has therefore been recognized as a serious disease. However, the precise mechanism of hepatocarcinogenesis during chronic HCV infection remains unclear.

Many experiments using cell culture systems have suggested the possibility that HCV core protein itself can modulate various cellular functions and can be directly linked to the development of HCV-related HCC.[5] For example, HCV core protein transforms rat embryo fibroblasts to a tumorigenic phenotype in cooperation with the H-*ras* oncogene,[6] suppresses *c-myc*-related apoptosis[7] and transcription of the *p53* gene,[8] interacts with a variety of proteins, including helicase, lymphotoxin-β receptor, or dead box protein, and modulates their functions.[9] We further established transgenic mouse lines carrying the HCV core gene, in which the core protein is constitutively expressed in the liver at levels similar to that found in chronic hepatitis C patients.[10] These mice exhibited multicentric hepatic adenomas, and developed HCCs in an age-dependent manner.[11] The livers of these mice were almost free of inflammation, necrosis and fibrosis,[10,11] suggesting that the core protein itself has a hepatocarcinogenic potential *in vivo*. However, the molecular mechanism of the development of HCC in the transgenic mice has not been fully understood.

In the livers of HCV core gene transgenic mice, an age-dependent increase in oxidative stress and resultant DNA damage were found,[12] and these effects may contribute to or facilitate the development of HCC. Another possible mechanism of hepatocarcinogenesis is continuous enhancement of hepatocyte proliferation. Cell proliferation and apoptosis are highly regulated processes for maintaining homeostasis in many organs, and during the carcinogenic process, sustained imbalance generally precedes cancer.[13,14] For example, in patients with chronic HCV infection, high hepatocyte proliferative activity relative to apoptosis may reliably predict a new development of HCC.[15] However, there is no information about whether or not hepatocyte proliferation accelerates persistently in mice carrying the HCV core gene, and no information about how the core protein promotes hepatocyte proliferation *in vivo*. In the current study, we began to examine changes in the parameters of hepatocyte proliferation and apoptosis in the transgenic mice.

Material and methods

Animals and treatments

HCV core gene transgenic mice on a C57BL/6N genetic background were produced as described earlier.[10] Because HCC developed preferentially in male transgenic mice,[11] 9- and 22-month-old male mice ($n = 8$ for either age group) were adopted. Sex- and age-matched nontransgenic mice ($n = 8$ for either age group) were used as controls. These mice were fed an ordinary diet and were treated in a specific pathogen-free state according to the institutional guidelines. For additional experiment, male wild-type mice fed a control diet containing 0.5% clofibrate for 2 weeks ($n = 8$) were used. All mice were killed by cervical dislocation and the livers were excised. When a hepatic tumor was present, it was removed and the remaining liver tissue was used. All experiments were performed in accordance with animal study protocols approved by the Shinshu University School of Medicine.

Abbreviations: AOX, acyl-CoA oxidase; CDK, cyclin-dependent kinase; DAB, 3,3'-diaminobenzidine; FITC, fluorescein isothiocyanate; HCC, hepatocellular carcinoma; HCV, hepatitis C virus; L-FABP, liver-type fatty acid-binding protein; NEFA, nonesterified fatty acid; PBS, phosphate-buffered saline; PCNA, proliferating cell nuclear antigen; PMSF, phenylmethylsulfonyl fluoride; PPAR, peroxisome proliferator-activated receptor; PT, peroxisomal thiolase; RXR, retinoid X receptor; SDS, sodium dodecyl sulfate; TUNEL, terminal deoxynucleotidyl transferase-mediated deoxyuridine triphosphate nick-end labeling.

***Correspondence to:** Department of Metabolic Regulation, Institute on Aging and Adaptation, Shinshu University Graduate School of Medicine, 3-1-1 Asahi, Matsumoto, 390-8621, Japan. Fax: +81-26-337-3094.
E-mail: naopi@hsp.md.shinshu-u.ac.jp

Received 2 May 2007; Accepted after revision 28 June 2007
DOI 10.1002/ijc.23056
Published online 31 August 2007 in Wiley InterScience (www.interscience.wiley.com).

Preparation of hepatocyte nuclear fraction

Approximately 200 mg of liver tissues was transferred to a chilled Dounce homogenizer (Wheaton, Milliville, NJ) and homogenized on ice by 30 strokes in 1.2 mL of nuclei buffer [300 mM sucrose in 10 mM Tris-HCl, pH 7.4, 15 mM NaCl, 5 mM $MgCl_2$ and 0.25 mM phenylmethylsulfonyl fluoride (PMSF)]. The homogenate was filtered through gauze and centrifuged at 4,500*g* for 5 min at 4°C. The resulting pellet was resuspended, layered over 2 mL of nuclei buffer containing 2 M sucrose, and centrifuged at 23,000*g* for 1 hr at 4°C. The pellet obtained after ultracentrifugation was resuspended in 250 μL of nuclei buffer and used as the nuclear fraction. Preparation of nuclear fraction from isolated hepatocytes was performed as described elsewhere.[16]

Immunoblot analysis

Protein concentration was measured colorimetrically by a BCA™ Protein Assay kit (Pierce, Rockford, IL). For analysis of fatty acid-metabolizing enzymes and protein, whole liver lysate (10–20 μg protein) was subjected to 10% sodium dodecyl sulfate (SDS)-polyacrylamide gel electrophoresis.[17] For analysis of other proteins, hepatocyte nuclear fraction (100 μg protein) or whole liver lysate (200–300 μg protein) was subjected to electrophoresis. After electrophoresis, the proteins were transferred to nitrocellulose membranes, which were incubated with the primary antibody, followed by alkaline phosphatase-conjugated goat anti-rabbit or anti-mouse IgG. The origin of the primary rabbit polyclonal antibodies against fatty acid-metabolizing enzymes and protein was described earlier.[17] For immunoblot analysis of peroxisome proliferator-activated receptor α (PPARα), a polyclonal anti-mouse antibody[18] or commercial antibody (Santa Cruz Biotechnology, Santa Cruz, CA) was used. The antibodies against cell-cycle regulators and oncogene products were purchased commercially (Santa Cruz Biotech.).[19] Equal loading of the protein obtained from whole liver lysate and nuclear fraction was confirmed by reprobing the membranes with an antibody against β-actin and histone H1, respectively. The band intensity of nuclear PPARα was quantified densitometrically, normalized to that of histone H1, and subsequently expressed as the fold changes relative to that of 9-month-old nontransgenic mice.

mRNA analysis

Total liver RNA was extracted with an RNeasy Mini Kit™ (Qiagen, Valencia, CA). Five microgram of RNA was electrophoresed on 1.1 M formaldehyde-containing 1% agarose gels and transferred to nylon membranes by capillary blotting in 20× SSC buffer (3 M NaCl and 300 mM sodium citrate, pH 7.0) overnight. The membranes were hybridized with ^{32}P-labeled cDNA probes. The blots were exposed to a phosphorimager screen cassette and were analyzed using a Molecular Dynamics Storm 860 Phosphorimager system (Sunnyvale, CA). The origin of the cDNA probes has been described elsewhere.[17–19] Northern blot of β-actin was used as the internal control. The blot intensity was quantified, normalized to that of β-actin and subsequently expressed as the fold changes relative to that of 9-month-old nontransgenic mice.

Pulse-label and pulse-chase experiment

Parenchymal hepatocytes were isolated from transgenic and control mice by the modified *in situ* perfusion method.[20] After perfusion with 0.05% collagenase solution (Wako, Osaka, Japan), the isolated hepatocytes were washed thrice by means of differential centrifugation and the dead cells removed by density gradient centrifugation on Percoll (Amersham Pharmacia Biotech, Buckinghamshire, UK). The live hepatocytes were washed and suspended in William's E medium containing 5% fetal bovine serum. When the viability of the isolated hepatocytes exceeded 85% as determined by the trypan blue exclusion test, the following experiments were conducted. The isolated hepatocytes were washed twice and incubated in methionine-free medium containing 5% dialyzed fetal bovine serum for 1 hr at 37°C. The medium was replaced with the same medium containing 300 μCi/mL of [^{35}S]methionine (Amersham Pharmacia Biotech.). After 3-hr of incubation, the labeled medium was changed to the standard medium and the preparation was chased for 4, 8 or 16 hr. The labeled cells were washed, homogenized and centrifuged for preparation of the nuclear fraction. The levels of radioactivity in the homogenates of the pulse-labeled preparations were similar between the transgenic and the nontransgenic mice, suggesting that the [^{35}S]methionine uptake capacity in the former hepatocytes is similar to that in the latter. The nuclear fraction was lysed in RIPA buffer [10 mM Tris-HCl, pH 7.4, 0.2% sodium deoxycholate, 0.2% Nonidet P-40, 0.1% SDS, 0.25 mM PMSF, 10 μg/mL aprotinin]. The lysate was incubated for 3 hr at 4°C with purified anti-PPARα antibody. The immune complexes were precipitated with *Staphylococcus aureus* protein A bound to agarose beads. After the precipitates had been washed in RIPA buffer, the labeled proteins were resolved by 10% SDS-polyacrylamide gel electrophoresis and visualized by autoradiography. The nuclear fractions of the pulse-labeled preparations were also used for immunoblot analysis of PPARα.

Affinity chromatography for PPARα complex

All procedures were performed at 4°C. The nuclear fraction from the mouse liver was mixed with a 4-fold volume of a solution containing 12.5 mM potassium phosphate, pH 7.5, 25 mM NaCl, 0.25% Tween 20 and 0.1 mM PMSF. The mixture was briefly sonicated with a microsonicator, the Powersonic Model 50 (Yamato, Tokyo, Japan), and then centrifuged at 100,000*g* for 20 min. The supernatant was applied to an immobilized anti-PPARα IgG column (1.0 × 4.0 cm^2), prepared with the Affigel HZ Immunoaffinity kit^R (Bio-Rad, Hercules, CA) and equilibrated with 10 mM potassium phosphate, pH 7.5, 20 mM NaCl and 0.2% Tween 20. The solution was again passed through the column and this was repeated at least thrice. The column was washed and the elution performed with 150 mM sodium citrate, pH 3.0, and 200 mM NaCl, in a total volume of 2 mL. The eluate was resolved by 10 and 15% SDS-polyacrylamide gel electrophoresis for PPARα and the HCV core protein, respectively. The core protein expressed in COS cells was used as a positive marker.[21] The monoclonal antibody against the core protein was purchased commercially (ViroGen, Watertown, MA).

Cytochemical staining of peroxisomes

Liver peroxisome proliferation was evaluated by using 3,3′-diaminobenzidine (DAB) staining for catalase according to the method of Novikoff and Goldfischer with minor modifications.[22] Small pieces of liver were fixed with 2% glutaraldehyde in 100 mM sodium cacodylate buffer, pH 7.2, for 3 hr at 4°C, rinsed with sodium cacodylate buffer and cut into 100-μm sections with a Lancer^R Vibratome 1000 (Lancer, Bridgeton, MO). These sections were then incubated for 1 hr at 37°C in the DAB reaction medium (0.2% DAB tetrahydrochloride in 50 mM propanediol, pH 9.7, 5 mM KCN, 0.05% H_2O_2) and postfixed with 1% OsO_4 in 100 mM sodium phosphate, pH 7.4 for 1 hr. The sections were dehydrated through a graded series of ethanol and acetone treatments and embedded in Epok 812 (Oken, Tokyo, Japan). One micrometer sections were prepared, counterstained with 0.1% toluidine blue solution and examined by light microscopy. For electron microscopic examination, 0.1-μm sections were cut with a diamond knife, collected on grid meshes, stained with lead citrate and uranyl acetate and visualized with a JEM 1200EX II electron microscope (JEOL, Tokyo, Japan) at an accelerating voltage of 80 keV.

Morphometry of hepatic peroxisomes

Morphometric analysis of DAB-stained peroxisomes was carried out using electron photomicrographs. For each mouse, 10 independent fields in the pericentral area of liver lobuli were photomicrographed at an original magnification of 4,000×. At this magnification, peroxisomes smaller than 450 nm were clearly

identified. Peroxisomes were easily detected because of their high contrast because of the positive DAB reaction. In each frame, the number of peroxisomal profiles and the area of each individual profile were determined. The numerical density and volume density of peroxisomes were calculated using the following equations: numerical density (number/μm^2) = $N_P/(A_T - A_{empty})$, and volume density (%) = $A_{TP}/(A_T - A_{empty}) \times 100$, where N_P is the peroxisome number in the test area, A_T is the test area, A_{empty} is the area of the vascular and biliary lumens and that of the hepatocyte nuclei and lipid droplets, and A_{TP} is the area of total peroxisomal profiles in the test area. The area was measured with a Luzex AP image analyzer (Nireco, Tokyo, Japan).

Immunofluorescence staining

Liver samples were fixed in 4% paraformaldehyde in phosphate-buffered saline (PBS), embedded in Tissue-Tek O.C.T compound™ (Sakura Finetek, Torrance, CA) and frozen. Frozen liver 5-μm sections were prepared, washed with PBS, blocked with bovine serum albumin for 1 hr and incubated overnight with rabbit polyclonal antibodies against cyclin D1 (1:50 dilution)[19] and PPARα (1:100 dilution),[18] and with mouse monoclonal antibody against proliferating cell nuclear antigen (PCNA) (1:100 dilution).[19] After 5 washes with PBS, these sections were incubated with fluorescein isothiocyanate (FITC)-conjugated goat anti-rabbit IgG (Jackson ImmunoResearch, West Grove, PA) or donkey anti-mouse IgG (Dako). The sections were mounted and viewed with an Olympus Fluoview confocal laser scanning microscope (Olympus, Tokyo, Japan). Two-thousand hepatocyte nuclei were examined for each mouse, and the number of hepatocyte nuclei stained with the antibodies against cyclin D1, PPARα and PCNA was counted and expressed as a percentage.

Assessment of apoptotic hepatocytes

Liver samples were cut into small pieces and then fixed in 4% paraformaldehyde in PBS. These samples were dehydrated, embedded in paraffin and cut into 4-μm sections. The terminal deoxynucleotidyl transferase-mediated deoxyuridine triphosphate nick-end labeling (TUNEL) assay was performed using a MEBSTAIN Apoptosis Kit II (Medical and Biological Laboratories, Nagoya, Japan). The number of apoptotic hepatocytes in 2,000 hepatocytes was counted for each mouse, and expressed as a percentage.

Other methods

Hepatic caspase 3 activity was measured as described elsewhere.[23] For analysis of the nuclear contents of nonesterified fatty acids (NEFAs), ~150 μL of the hepatocyte nuclear fraction, containing 1–2 mg of protein, was treated with a microsonicator. Lipid extraction was performed according to a modification of the method developed by Folch *et al.*[24] and the nuclear content of NEFAs was measured with a *NEFA* C-test kit™ (Wako).

Statistical analysis

Statistical analysis was performed by means of Student's *t*-test. The results are expressed as the mean ± standard deviation. A probability value of less than 0.05 was considered to be statistically significant.

Results

Accelerated hepatocyte proliferation in HCV core gene transgenic mice

To evaluate hepatocyte proliferative activity, PCNA-positive hepatocytes were counted in male transgenic mice and nontransgenic mice. Although hepatic inflammation and hepatocyte necrosis were not detected in either group, the numbers of PCNA-positive hepatocytes were significantly increased in the 9-month-old transgenic mice compared with the 9-month-old nontransgenic mice (Fig. 1*a*). The increase was more significant in the 22-month-old transgenic mice (Fig. 1*a*). The numbers of PCNA-positive hepatocytes in the 22-month-old transgenic mice corresponded with those in HCV polyprotein-expressing transgenic mice with HCC.[25] On the other hand, the parameters of apoptosis, *i.e.*, the numbers of TUNEL-positive hepatocytes and hepatic caspase 3 activity, remained unchanged between the 2 groups at the same ages (Figs. 1*b* and 1*c*). These results suggest that spontaneous hepatocyte proliferation occurs as early as the age of 9 months and persists for a long time in HCV core gene transgenic mice.

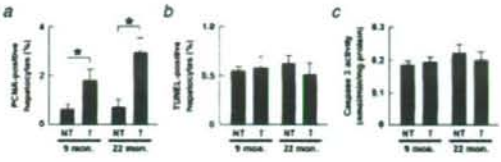

FIGURE 1 – Increase in hepatocyte proliferative activity. (*a*) The number of PCNA-positive hepatocytes. Two-thousand hepatocyte nuclei were examined for each mouse, and the number stained with anti-PCNA antibody was counted. Results are expressed as the mean ± standard deviation ($n = 8$). *, $p < 0.05$ between the transgenic mice and the nontransgenic mice; NT, nontransgenic mice; T, transgenic mice; 9 mon, 9-month-old mice; 22 mon, 22-month-old mice. (*b*) The number of apoptotic hepatocytes. The number of TUNEL-positive hepatocytes in 2,000 hepatocytes was determined for each mouse. Results are expressed as the mean ± standard deviation ($n = 8$). (*c*) Caspase 3 activity. Results are expressed as the mean ± standard deviation ($n = 8$).

Simultaneous induction of cell-cycle regulators and oncogene products in HCV core gene transgenic mouse livers

To examine the changes in the expression of proteins associated with hepatocyte division, the livers of the 9- and 22-month-old mice were subjected to immunoblot analysis. The levels of many proteins including cell-cycle regulators [cyclin-dependent kinase (CDK) 1, 2 and 4, cyclin D1 and E, and PCNA], and oncogene products (c-Myc, c-Fos and c-Ha-Ras) were significantly higher in the 22-month-old transgenic mice than in the control mice (Fig. 2). The levels of CDK inhibitors such as p16 and p21 were similar between the 2 groups. Similar results were obtained from the 9-month-old transgenic mice (data not shown). Time course changes in the expression of key G1-S checkpoint regulators, cyclin D1 and CDK4, are shown in Figure 3*a*. The simultaneous increase in the expression of cyclin D1 and CDK4 in the transgenic mice was continuous and more pronounced with age. Northern blot analysis revealed that the increase of these proteins occurred at the transcriptional level (Figs. 3*b* and 3*c*). Thus, these results reveal that various proteins which accelerate cell-cycle progression were induced simultaneously, persistently and age-dependently in the transgenic mice.

Correlative induction of PPARα targets in HCV core gene transgenic mouse livers

As shown in Figure 2, the expression of many kinds of cell-cycle regulators and oncogene products is known to be induced by the functional activation of PPARα.[19,26–30] To investigate whether PPARα is activated in the livers of transgenic mice, the expression of representative PPARα target genes,[30] acyl-CoA oxidase (AOX), peroxisomal thiolase (PT) and liver-type fatty acid-binding protein (L-FABP), was examined. As demonstrated in Figure 3*a*, the levels of AOX, PT, and L-FABP were increased in the 9-month-old transgenic mice compared with the nontransgenic mice, and the increase was more pronounced in the 22-month-old transgenic mice. Northern blot analysis demonstrated that the increase in these PPARα targets was based on the increase in the transcriptional activity (Figs. 3*b* and 3*c*). The increase in the

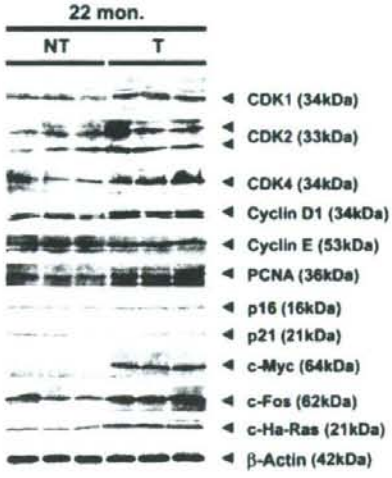

FIGURE 2 – Immunoblot analysis of cell-cycle regulators and oncogene products. Whole liver lysate (200 μg) was loaded in each lane. The band of β-actin was used as the loading control. The apparent molecular weight is indicated in parentheses. 22 mon, 22-month-old mice; NT, nontransgenic mice; T, transgenic mice.

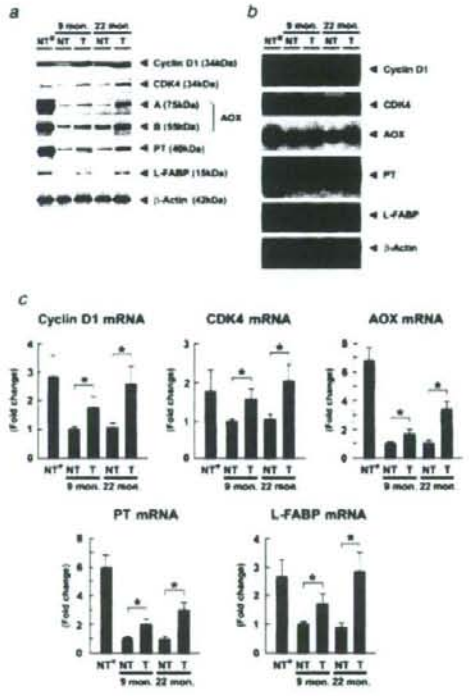

FIGURE 3 – Analysis of PPARα-regulated proteins. (*a*) Immunoblot analysis of cell-cycle regulators and fatty acid-metabolizing enzymes and proteins. Since no significant individual differences in the same mouse group were found in the preliminary experiments, 10 mg of liver pieces prepared from each mouse (n = 8/group) was mixed and homogenized. Whole liver lysate (200 μg for cyclin D1 and CDK4, and 20 μg for others) was loaded in each lane. The band of β-actin was used as the loading control. Results are representative of 4 independent experiments. The apparent molecular weight is indicated in parentheses. 9 mon, 9-month-old mice; 22 mon, 22-month-old mice; NT, nontransgenic mice; T, transgenic mice; NT*, nontransgenic mice treated with a control diet containing 0.5% clofibrate for 2 weeks; A and B, full-length and truncated AOX, respectively. (*b*) Northern blot analysis concerning the proteins in (*a*). Ten milligram of liver pieces from each mouse (n = 8/group) was mixed and homogenized, and total liver RNA was extracted. Hepatic RNA (5 μg) was separated on a denaturing gel, transferred to membranes and hybridized with the indicated ^{32}P-labeled cDNA probes. The blot of β-actin was used as the internal control. Results are representative of 4 independent experiments. (*c*) Quantification of hepatic mRNA levels. The mRNA level was quantified using a phosphorimager, normalized to that of β-actin, and subsequently normalized to that of 9-month-old nontransgenic mice. Results were obtained from 4 independent experiments and expressed as the mean ± standard deviation. Abbreviations are identical with those in (*b*). *, $p < 0.05$ between the transgenic mice and the nontransgenic mice.

mRNA expression of AOX, PT and L-FABP corresponded exactly with that of cyclin D1 or CDK4 (Figs. 3*b* and 3*c*). Therefore, these results demonstrate the strong correlation between continuous and age-dependent induction of cell-cycle regulators and functional activation of PPARα in these transgenic mice. Furthermore, the induction of these 5 proteins was also observed in wild-type mice treated with clofibrate, a potent PPARα activator; however, the degree of the induction of AOX and PT in the transgenic mice was smaller than that in the clofibrate-treated wild-type mice (Fig. 3), suggesting that the PPARα activation found in the transgenic mice was not as intense as that in the mice treated with clofibrate.

Histological evaluation of PPARα activation

An increase in the numbers of peroxisomes is associated with PPARα activation.[18] To determine whether peroxisome proliferation occurs in the HCV core gene transgenic mice, cytochemical staining for peroxisomal catalase was performed. A scattered distribution of hepatocytes with numerous peroxisomes was observed in the 9-month-old transgenic mice (Fig. 4*a*). Such hepatocytes were also found in the 22-month-old transgenic mouse livers (Fig. 4*a*). In contrast, almost all of the hepatocytes in the clofibrate-treated mice showed significant peroxisome proliferation (Fig. 4*a*). To quantitatively evaluate the degree of peroxisome proliferation, morphometric analysis of peroxisomes was conducted. The numerical density and volume density were significantly increased in the transgenic mice compared with those in the nontransgenic mice (Fig. 4*b*). The volume density, the most reliable parameter of peroxisome proliferation, was increased age-dependently in the transgenic mice, but the degree of the increase was not as prominent as that observed in mice with clofibrate administration (Fig. 4*b*). The finding that only some hepatocytes in the transgenic mice presented a marked peroxisome proliferation (Fig. 4*a*) is noteworthy, since it seems to correlate with the finding that intense expression of the core protein was observed only in particular hepatocytes.[10] These histological analyses reveal that spontaneous, continuous and age-dependent peroxisome proliferation and PPARα activation occur heterogeneously in the transgenic mouse livers, which is different from the response observed in the mice receiving clofibrate treatment.

Appearance of PPARα-, and cyclin D1-positive hepatocytes

We tried to detect abnormal hepatocytes to clarify the mechanism of hepatocarcinogenesis in the transgenic mice. On PPARα immunofluorescence staining, PPARα was primarily detected in the cytoplasm of the nontransgenic mice and the clofibrate-administered mice. Some hepatocytes having nuclei positively stained

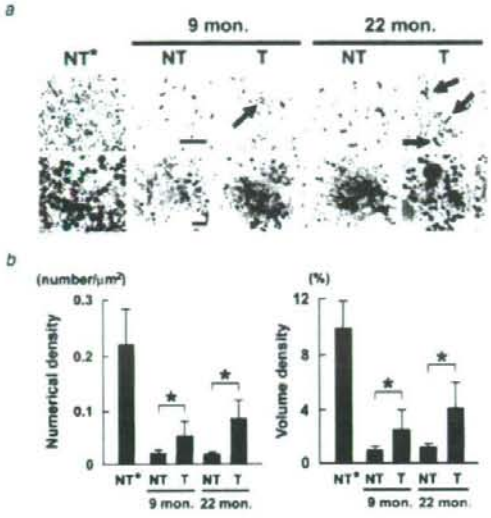

FIGURE 4 – Cytochemical staining for hepatic peroxisomes. (*a*) Light and electron photomicrographs of DAB-stained liver tissues. Peroxisomes are detected as darkly stained particles. The arrows in upper panels indicate hepatocytes showing profound peroxisome proliferation. The bars in the light and electron photomicrographs of 9-month-old nontransgenic mice indicate 50 and 2 μm, respectively. 9 mon, 9-month-old mice; 22 mon, 22-month-old mice; NT, nontransgenic mice; T, transgenic mice; NT*, nontransgenic mice treated with a control diet containing 0.5% clofibrate for 2 weeks. (*b*) Morphometric analysis of hepatic peroxisomes. The number of peroxisomes and the area of each individual peroxisome profile were measured in 10 photomicrographs for each mouse, and morphometric parameters such as numerical density and volume density were calculated. Results are expressed as the mean ± standard deviation ($n = 8$). Abbreviations are identical with those in (*a*). *, $p < 0.05$ between the transgenic mice and the nontransgenic mice.

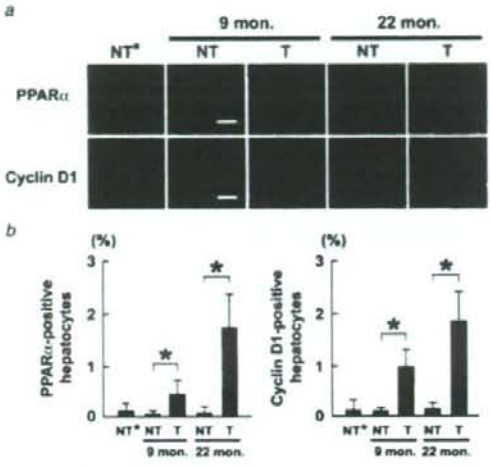

FIGURE 5 – Immunofluorescence staining for PPARα and cyclin D1. (*a*) Immunofluorescence staining using antibodies against PPARα and cyclin D1. The bars in the photomicrographs of 9-month-old nontransgenic mice indicate 50 μm. 9 mon, 9-month-old mice; 22 mon, 22-month-old mice; NT, nontransgenic mice; T, transgenic mice; NT*, nontransgenic mice treated with a control diet containing 0.5% clofibrate for 2 weeks. (*b*) The number of PPARα-, or cyclin D1-positive hepatocytes. Two-thousand hepatocyte nuclei were examined for each mouse, and the number of nuclei intensively stained with anti-PPARα or anti-cyclin D1 antibody was counted. Results are expressed as the mean ± standard deviation ($n = 8$). Abbreviations are identical with those of (*a*). *, $p < 0.05$ between the transgenic mice and the nontransgenic mice.

by anti-PPARα antibody were detected only in the transgenic mice (Fig. 5*a*). Similar to the case of PPARα, the hepatocytes having nuclei stained intensively by anti-cyclin D1 antibody were found only in the transgenic mice (Fig. 5*a*). A few hepatocytes stained by anti-CDK4 antibody were also observed only in the transgenic mice (data not shown). The frequency of appearance of PPARα-, or cyclin D1-positive hepatocytes was increased with age (Figs. 5*a* and 5*b*). Thus, the appearance of these specific hepatocytes in the transgenic mice seemed to be, at least in part, associated with sustained, age-dependent and heterogeneous PPARα activation in the transgenic mice.

Changes in PPARα levels

Since the expression of PPARα is known to be enhanced by its activation,[18,30] the quantitative change in PPARα was evaluated. The nuclear PPARα level in the transgenic mice was increased age-dependently, as expected (Figs. 6*a*, upper panel and 6*b*), but the PPARα level in the whole liver lysate remained unchanged (data not shown). The increase in nuclear PPARα in the transgenic mice was smaller than that in the clofibrate-treated wild-type mice (Figs. 6*a*, upper panel and 6*b*). Northern blot analysis revealed a higher PPARα mRNA level in the clofibrate-treated mice than in the controls, although this parameter in the transgenic mouse groups of each age was similar to that in the controls (Figs. 6*a*, lower panel and 6*b*). These results indicate that the increase in nuclear PPARα in the transgenic mice occurs mainly at the post-transcriptional level, which is distinct from that observed in the clofibrate-treated wild-type mice.

Stabilization of PPARα through a possible interaction with HCV core protein in hepatocyte nuclei

The increased stability of PPARα in hepatocyte nuclei is thought to be one of the possible causes of a disproportional increase in the nuclear PPARα level. To examine this possibility, a pulse-chase experiment was performed using isolated hepatocytes. The half-life of nuclear PPARα was ~7 hr in the control mice and 12.5 hr in the transgenic mice (Fig. 7*a*). In addition, the intensity of the labeled PPARα band (P in Fig. 7*a*, upper panels) in the control mice was similar to that in the transgenic mice. The finding that the [^{35}S]methionine uptake in the hepatocytes from the control mice was similar to that from the transgenic mice suggests that the increase in nuclear PPARα in the hepatocytes from the transgenic mice (Fig. 7*a*, lower right panel), as well as that *in vivo* (Fig. 6*a*, upper panel), is not because of the increased PPARα transfer into the nucleus.

In the transgenic mice, HCV core protein accumulated in the nuclei, as evidenced by immunoelectron microscopy,[11] suggesting a possible interaction of the core protein with PPARα in the nuclei. We therefore examined this possibility by anti-PPARα IgG affinity chromatography. When proteins combining with PPARα in hepatocyte nuclei were subjected to immunoblot analysis, the core protein was clearly detected (Fig. 7*b*). This result suggests the possibility of complex formation between the HCV core protein and PPARα, which is consistent with an interaction of the core protein with retinoid X receptor (RXR) α,[31] an essential heterodimeric partner of PPARα.[32] Thus, HCV core protein may

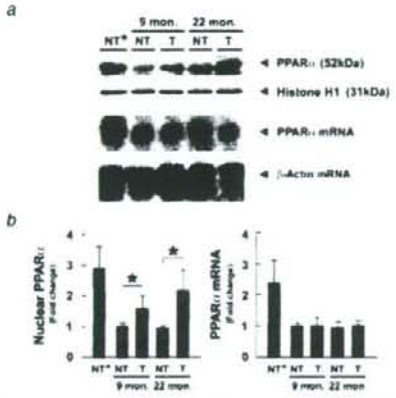

FIGURE 6 – Analysis of PPARα. (*a*) (Upper panels) Immunoblot analysis of nuclear PPARα. Since few individual differences in the same mouse group were found in the preliminary experiments, 30 mg of liver pieces from each mouse (n = 8/group) was mixed and homogenized to prepare the nuclear fraction. One-hundred microgram of nuclear protein was separated on 10% SDS-polyacrylamide gel, transferred to nitrocellulose membranes and reacted with antibody against PPARα. The band of histone H1 was used as the loading control. Results are representative of 4 independent experiments. The apparent molecular weight is indicated in parentheses. 9 mon, 9-month-old mice; 22 mon, 22-month-old mice; NT, nontransgenic mice; T, transgenic mice; NT*, nontransgenic mice treated with a control diet containing 0.5% clofibrate for 2 weeks. (Lower panels) Northern blot analysis of PPARα. A sample used in Figure 3*b* was adopted. Hepatic RNA (5 μg) was electrophoresed and hybridized with cDNAs for PPARα and β-actin, respectively. Results are representative of 4 independent experiments. (*b*) Quantification of nuclear PPARα levels and PPARα mRNA levels. The nuclear PPARα level was quantified densitometrically and normalized to the histone H1 level. The mRNA level of PPARα was quantified using a phosphorimager and normalized to that of β-actin. Values were subsequently normalized to those of 9-month-old nontransgenic mice. Results were obtained from 4 independent experiments and expressed as the mean ± standard deviation. Abbreviations are identical with those in (*a*). *, $p < 0.05$ between the transgenic mice and the nontransgenic mice.

directly or indirectly affect the stability of PPARα in hepatocyte nuclei.

Increase in PPARα ligands

PPARα is a ligand-activated transcription factor. Since the transgenic mice were fed a standard laboratory chow, endogenous substances such as NEFAs would serve as ligands of PPARα[33]; therefore, the contents of NEFAs in hepatocyte nuclei were compared between the 2 groups. The levels of NEFAs in hepatocyte nuclei in the transgenic mice were ~5 times higher than those in the control mice at the same age (Fig. 7*c*). This could account for the higher activation of PPARα in the transgenic mice than in the controls.

Discussion

A large number of variables are involved in the induction of HCC by HCV core protein. While the precise mechanism underlying hepatocarcinogenesis in HCV core gene transgenic mice cannot be fully elucidated from this study, our results could provide some clues to explain this phenomenon. We found spontaneous, persistent, age-dependent and heterogeneous PPARα activation in the transgenic mouse livers for the first time. This study thus advances our understanding of the association

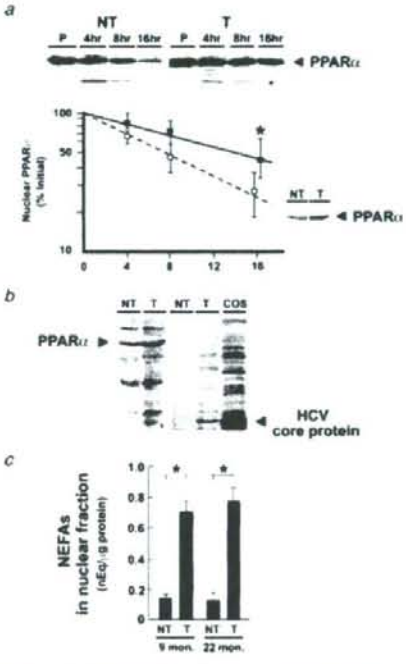

FIGURE 7 – Analyses of PPARα stability, interaction between PPARα with the core protein in hepatocyte nuclei, and nuclear contents of NEFAs. (*a*) Pulse-label and pulse-chase experiments for nuclear PPARα using isolated mouse hepatocytes. (Upper panels) Labeled PPARα bands on X-ray film. Pulse-label and pulse-chase experiments were performed as described in the Material and methods. NT, nontransgenic mice; T, transgenic mice; P, pulse-label; 4, 8, 16 hr, pulse-chase for 4, 8, 16 hr, respectively. (Lower left panel) Intensity plot of PPARα in 5 independent experiments. Values are normalized as a percentage of the values of the pulse-labeled band and expressed as the mean ± standard deviation. Open square, nontransgenic mice; black square, transgenic mice; *, $p < 0.05$ between the transgenic mice and the nontransgenic mice. (Lower right panel) Immunoblot analysis of an isolated hepatocyte nuclear fraction. NT, nontransgenic mice; T, transgenic mice. (*b*) Interaction between PPARα and HCV core protein in the nucleus. (Left panel) Immunoblot analysis (PPARα) of the eluate on anti-PPARα IgG affinity column chromatography. (Right panel) Immunoblot analysis (HCV core protein) of the same eluate. NT, nontransgenic mice; T, transgenic mice; COS, HCV core protein-overexpressing COS cell lysate. (*c*) Nuclear contents of NEFAs. The levels of NEFAs were measured using a hepatocyte nuclear fraction. Results are expressed as the mean ± standard deviation (n = 8). *, $p < 0.05$ between the transgenic mice and the nontransgenic mice; NT, nontransgenic mice; T, transgenic mice; 9 mon, 9-month-old mice; 22 mon, 22-month-old mice.

between HCV core protein-mediated hepatocarcinogenesis and persistent PPARα activation.

Hepatocyte proliferation is influenced by various factors, such as mitogenic chemicals, cytokines, growth factors and transcription factors. It has been reported that various kinds of cell-cycle regulators and oncogene products are induced by PPARα activation.[19,26–30] In particular, cyclin D1, CDK4, PCNA and c-Myc are potent and critical regulators of the G1-S checkpoint and cell-cycle progression,[13,14] and aberrant expression of these proteins is frequently detected in HCV-related HCC.[34–37] These key regulators are known to be induced in a PPARα-dependent manner in mice[19,30]; the continuous induction of these proteins and the

resultant acceleration of hepatocyte proliferation found in the transgenic mice may be attributed to persistent PPARα activation. In the current study, we demonstrated that there was a great variety of the intensity of PPARα activation among different hepatocytes (Fig. 4). This persistent and heterogeneous PPARα activation found especially in the transgenic mice may be linked with the age-dependent and multicentric hepatocarcinogenesis induced by the core protein.

It is well-known that the long-term administration of potent peroxisome proliferators such as fibrate drugs can induce hepatocarcinogenesis in rodents.[29] The findings observed in the transgenic mice markedly differ from those in mice with long-term treatment of peroxisome proliferators in several ways. Namely, the transgenic mice show no intense increase in AOX and PT (Fig. 3), no increase in PPARα mRNA (Fig. 6), heterogeneous peroxisome proliferation (Fig. 4) and age-dependent emergence of hepatocytes having nuclei stained intensively by anti-PPARα or anti-cyclin D1 antibody (Fig. 5). Therefore, the mode of PPARα activation and the mechanism of hepatocarcinogenesis caused by HCV core protein expression are indeed unique.

One of the mechanisms involved in the core protein-specific PPARα activation in mice is stabilization of PPARα in hepatocyte nuclei through a possible interaction with the core protein. In cultured cells expressing the core protein, it has been demonstrated that the core protein interacts with the PPARα-RXRα heterodimer and enhances the transcriptional activation mediated by PPARα regardless of the presence or absence of its ligands.[31] Since PPARα is ubiquitinated and degraded *via* the proteasome pathway,[38] it may be postulated that HCV core protein directly or indirectly influences the degradation pathway. It has been reported that the core protein binds to the proteasome activator PA28γ[39] which is known to combine with steroid receptor coactivator-3 and to accelerate its degradation.[40] Another possible mechanism is an increase in NEFAs in hepatocyte nuclei. The PPARα activation induced by the core protein enhances the expression of L-FABP,[30] which serves as a transporter of NEFAs into nuclei. Indeed, real-time confocal and multiphoton laser scanning microscopy has shown that L-FABP expression significantly increased the total uptake of medium- and long-chain fluorescent fatty acids into the nuclei of living cells.[41] Thus, increased L-FABP expression may facilitate the shuttling of NEFAs into hepatocyte nuclei for donating NEFAs to PPARα, leading to PPARα activation and further increase in L-FABP expression. Moreover, the binding of ligands causes conformational alternation of PPARα[42] and further stabilizes it in nuclei,[32] resulting in synergistic PPARα activation. Therefore, these findings concerning spontaneous and persistent PPARα activation induced by the core protein enable us to partially explain the precise molecular mechanism of hepatocarcinogenesis in HCV core gene transgenic mice.

The results obtained from the current study are consistent with the findings observed in chronically HCV-infected patients in several ways. That is, like the transgenic mice in the present study, chronically HCV-infected patients have been reported to show accelerated hepatocyte proliferation,[43] an increase in CDK4, cyclin D1 and E, PCNA, c-Myc and c-Fos,[34–37] and multicentric appearance of HCC.[44] Furthermore, it has been reported that a massive proliferation of peroxisomes was found in human non-tumorous liver tissue adjacent to HCC.[45] Thus the earlier findings, including the unique function of HCV core protein *in vivo* and the diverse and significant roles of PPARα, may help to partially understand the onset and development of HCC in patients with chronic HCV infection. It has been demonstrated that the function of hepatic PPARα was impaired in patients with chronic HCV infection,[46] which is different from our results. Since HCC had not yet developed in the patients in the report, this discrepancy might derive from differences in the stage of the hepatocarcinogenic process.

The interpretation based on persistent activation of PPARα pertains to only one possible mechanism of hepatocarcinogenesis induced by the effects of HCV core protein. We cannot rule out the presence of other mechanisms. The exact relationship between PPARα activation and hepatocarcinogenesis may be elucidated by additional experiments in which PPARα activation is continuously inhibited in the same transgenic mice. Furthermore, the exact relationship may be confirmed when PPARα-null mice bearing the core protein gene do not represent development of HCC.

In conclusion, we demonstrated for the first time that spontaneous, persistent, age-dependent and heterogeneous activation of PPARα occurred in HCV core protein transgenic mice and caused continuous enhancement of hepatocyte proliferation, which may have contributed to the age-dependent and multicentric hepatocarcinogenesis observed in these mice. In addition, we observed nuclear stabilization of PPARα and an increase in NEFAs in the hepatocyte nuclei of the transgenic mice, which may have resulted in the HCV core protein-specific PPARα activation.

References

1. Kiyosawa K, Tanaka E, Sodeyama T. Hepatitis C virus and hepatocellular carcinoma. In: Reesink HW, ed. Hepatitis C virus: Current Studies in Hematology & Blood Transfusion, vol. 62. Basel: Karger, 1998.161–180.
2. Saito I, Miyamura T, Ohbayashi A, Harada H, Katayama T, Kikuchi S, Watanabe Y, Koi S, Onji M, Ohta Y, Choo QL, Houghton M, et al. Hepatitis C virus infection is associated with the development of hepatocellular carcinoma. Proc Natl Acad Sci USA 1990;87:6547–49.
3. Tanaka Y, Hanada K, Mizokami M, Yeo AE, Shih JW, Gojobori T, Alter HJ. A comparison of the molecular clock of hepatitis C virus in the United States and Japan predicts that hepatocellular carcinoma incidence in the United States will increase over the next two decades. Proc Natl Acad Sci USA 2002;99:15584–89.
4. Kiyosawa K, Umemura T, Ichijo T, Matsumoto A, Yoshizawa K, Gad A, Tanaka E. Hepatocellular carcinoma: recent trends in Japan. Gastroenterology 2004;127:S17–S26.
5. Watashi K, Shimotohno K. The roles of hepatitis C virus proteins in modulation of cellular functions: a novel action mechanism of the HCV core protein on gene regulation by nuclear hormone receptors. Cancer Sci 2003;94:937–43.
6. Ray RB, Lagging LM, Meyer K, Ray R. Hepatitis C virus core protein cooperates with *ras* and transforms primary rat embryo fibroblasts to tumorigenic phenotype. J Virol 1996;70:4438–43.
7. Ray RB, Meyer K, Ray R. Suppression of apoptotic cell death by hepatitis C virus core protein. Virology 1996;226:176–82.
8. McLauchlan J. Properties of the hepatitis C virus core protein: a structural protein that modulates cellular processes. J Viral Hepat 2000; 7:2–14.
9. Tellinghuisen TL, Rice CM. Interaction between hepatitis C virus proteins and host cell factors. Curr Opin Microbiol 2002;5:419–27.
10. Moriya K, Yotsuyanagi H, Shintani Y, Fujie H, Ishibashi K, Matsuura Y, Miyamura T, Koike K. Hepatitis C virus core protein induces hepatic steatosis in transgenic mice. J Gen Virol 1997;78:1527–31.
11. Moriya K, Fujie H, Shintani Y, Yotsuyanagi H, Tsutsumi T, Ishibashi K, Matsuura Y, Kimura S, Miyamura T, Koike K. The core protein of hepatitis C virus induces hepatocellular carcinoma in transgenic mice. Nat Med 1998;4:1065–7.
12. Moriya K, Nakagawa K, Santa T, Shintani Y, Fujie H, Miyoshi H, Tsutsumi T, Miyazawa T, Ishibashi K, Horie T, Imai K, Todoroki T, et al. Oxidative stress in the absence of inflammation in a mouse model for hepatitis C virus-associated hepatocarcinogenesis. Cancer Res 2001;61:4365–70.
13. Sherr CJ. Cancer cell cycles. Science 1996;274:1672–7.
14. Vousden KH, Evan GI. Proliferation, cell cycle and apoptosis in cancer. Nature 2001;411:342–8.
15. Donato MF, Arosio E, Del Ninno E, Ronchi G, Lampertico P, Morabito A, Balestrieri MR, Colombo M. High rates of hepatocellular carcinoma in cirrhotic patients with high liver cell proliferative activity. Hepatology 2001;34:523–8.
16. Yasui K, Wakita T, Tsukiyama-Kohara K, Funahashi S-I, Ichikawa M, Kajita T, Moradpour D, Wands JR, Kohara M. The native form and maturation process of hepatitis C virus core protein. J Virol 1998;72:6048–55.
17. Aoyama T, Peters JM, Iritani N, Nakajima T, Furihata K, Hashimoto T, Gonzalez FJ. Altered constitutive expression of fatty acid-metabo-

lizing enzymes in mice lacking the peroxisome proliferator-activated receptor α (PPARα). J Biol Chem 1998;273:5678–84.
18. Lee SS, Pineau T, Drago J, Lee EJ, Owens JW, Kroetz DL, Fernandez-Salguero PM, Westphal H, Gonzalez FJ. Targeted disruption of the α isoform of the peroxisome proliferator-activated receptor gene in mice results in abolishment of the pleiotropic effects of peroxisome proliferators. Mol Cell Biol 1995;15:3012–22.
19. Peters JM, Aoyama T, Cattley RC, Nobumitsu U, Hashimoto T, Gonzalez FJ. Role of peroxisome proliferator-activated receptor α in altered cell cycle regulation in mouse liver. Carcinogenesis 1998; 19:1989–94.
20. Ni R, Tomita Y, Matsuda K, Ichihara A, Ishimura K, Ogasawara J, Nagata S. Fas-mediated apoptosis in primary cultured mouse hepatocytes. Exp Cell Res 1994;215:332–7.
21. Harada S, Watanabe Y, Takeuchi K, Suzuki T, Katayama T, Takebe Y, Saito I, Miyamura T. Expression of processed core protein of hepatitis C virus in mammalian cells. J Virol 1991;65:3015–21.
22. Novikoff AB, Goldfischer S. Visualization of peroxisomes (microbodies) and mitochondria with diaminobenzidine. J Histochem Cytochem 1969;17:675–80.
23. Gurtu V, Kain SR, Zhang G. Fluorometric and colorimetric detection of caspase activity associated with apoptosis. Anal Biochem 1997; 251:98–102.
24. Folch J, Lees M, Sloane Stanley GH. A simple method for the isolation and purification of total lipids from animal tissues. J Biol Chem 1957;226:497–509.
25. Furutani T, Hino K, Okuda M, Gondo T, Nishina S, Kitase A, Korenaga M, Xiao SY, Weinman SA, Lemon SM, Sakaida I, Okita K. Hepatic iron overload induces hepatocellular carcinoma in transgenic mice expressing the hepatitis C virus polyprotein. Gastroenterology 2006;130:2087–98.
26. Cherkaoui-Malki M, Lone YC, Corral-Debrinski M, Latruffe N. Differential proto-oncogene mRNA induction from rats treated with peroxisome proliferators. Biochem Biophys Res Commun 1990; 173:855–61.
27. Ledwith BJ, Johnson TE, Wagner LK, Pauley CJ, Manam S, Galloway SM, Nichols WW. Growth regulation by peroxisome proliferators: opposing activities in early and late G1. Cancer Res 1996; 56:3257–64.
28. Rininger JA, Goldsworthy TL, Babishi JG. Time course comparison of cell-cycle protein expression following partial hepatectomy and WY14,643-induced hepatic cell proliferation in F344 rats. Carcinogenesis 1997;18:935–41.
29. Peters JM, Cheung C, Gonzalez FJ. Peroxisome proliferator-activated receptor-α and liver cancer: where do we stand? J Mol Med 2005; 83:774–85.
30. Mandard S, Muller M, Kersten S. Peroxisome proliferator-activated receptor α target genes. Cell Mol Life Sci 2004;61:393–416.
31. Tsutsumi T, Suzuki T, Shimoike T, Suzuki R, Moriya K, Shintani Y, Fujie H, Matsuura Y, Koike K, Miyamura T. Interacton of hepatitis C virus core protein with retinoid X receptor α modulates its transcriptional activity. Hepatology 2002;35:937–46.
32. Tanaka N, Hora K, Makishima H, Kamijo Y, Kiyosawa K, Gonzalez FJ, Aoyama T. In vivo stabilization of nuclear retinoid X receptor α in the presence of peroxisome proliferator-activated receptor α. FEBS Lett 2003;543:120–4.
33. Desvergne B, Wahli W. Peroxisome proliferator-activated receptors: nuclear control of metabolism. Endocr Rev 1999;20:649–88.
34. Ito Y, Sasaki Y, Horimoto M, Wada S, Tanaka Y, Kasahara A, Ueki T, Hirano T, Yamamoto H, Fujimoto J, Okamoto E, Hayashi N, et al. Activation of mitogen-activated protein kinases/extracellular signal-regulated kinases in human hepatocellular carcinoma. Hepatology 1998;27:951–8.
35. Masahi T, Shiratori Y, Rengifo W, Igarashi K, Yamagata M, Kurokohchi K, Uchida N, Miyauchi Y, Yoshiji H, Watanabe S, Omata M, Kuriyama S. Cyclins and cyclin-dependent kinases: comparative study of hepatocellular carcinoma versus cirrhosis. Hepatology 2003;37:534–43.
36. Nardone G, Romano M, Calabro A, Pedone PV, de Sio I, Persico M, Budillon G, Bruni CB, Riccio A, Zarrilli R. Activation of fetal promoters of insulin-like growth factors II gene in hepatitis C virus-related chronic hepatitis, cirrhosis, and hepatocellular carcinoma. Hepatology 1996;23:1304–12.
37. Kawate S, Fukusato T, Ohwada S, Watanuki A, Morishita Y. Amplification of *c-myc* in hepatocellular carcinoma: correlation with clinicopathologic features, proliferative activity and p53 overexpression. Oncology 1999;57:157–63.
38. Genini D, Catapano CV. Control of peroxisome proliferator-activated receptor fate by the ubiquitin-proteasome system. J Recept Signal Transduct Res 2006;26:679–92.
39. Moriishi K Okabayashi T, Nakai K, Moriya K, Koike K, Murata S, Chiba T, Tanaka K, Suzuki R, Suzuki T, Miyamura T, Matsuura Y. Proteasome activator PA28γ-dependent nuclear retention and degradation of hepatitis C virus core protein. J Virol 2003;77:10237–49.
40. Li X, Lonard D, Jung SY, Malovannaya A, Feng Q, Qin J, Tsai SY, Tsai M, O'Malley BW. The SRC-3/AIB1 coactivator is degraded in a ubiquitin- and ATP-independent manner by the REGγ proteasome. Cell 2006;124:381–92.
41. Huang H, Starodub O, McIntosh A, Kier AB, Schroeder F. Liver fatty acid-binding protein targets fatty acids to the nucleus. Real time confocal and multiphoton fluorescence imaging in living cells. J Biol Chem 2002;277:29139–51.
42. Dowell P, Peterson VJ, Zabriskie TM, Leid M. Ligand-induced peroxisome proliferator-activated receptor α conformational change. J Biol Chem 1997;272:2013–20.
43. Farinati F, Cardin R, Fiorentino M, D'Errico A, Grigioni W, Cecchetto A, Naccarato R. Imbalance between cytoproliferation and apoptosis in hepatitis C virus related chronic liver disease. J Viral Hepat 2001;8:34–40.
44. Oikawa T, Ojima H, Yamasaki S, Takayama T, Hirohashi S, Sakamoto M. Multistep and multicentric development of hepatocellular carcinoma: histological analysis of 980 resected nodules. J Hepatol 2005;42:225–9.
45. Litwin JA, Beier K, Volkl A, Hofmann WJ, Fahimi HD. Immunocytochemical investigation of catalase and peroxisomal lipid β-oxidation enzymes in human hepatocellular tumors and liver cirrhosis. Virchows Arch 1999;435:486–95.
46. Dharancy S, Malapel M, Perlemuter G, Roskams T, Cheng Y, Dubuquoy L, Podevin P, Conti F, Canva V, Philippe D, Gambiez L, Mathurin P, et al. Impaired expression of the peroxisome proliferator-activated receptor α during hepatitis C virus infection. Gastroenterology 2005;128:334–2.

PPARα activation is essential for HCV core protein–induced hepatic steatosis and hepatocellular carcinoma in mice

Naoki Tanaka,[1,2] Kyoji Moriya,[3] Kendo Kiyosawa,[2] Kazuhiko Koike,[3] Frank J. Gonzalez,[4] and Toshifumi Aoyama[1]

[1]Department of Metabolic Regulation, Institute on Aging and Adaptation, Shinshu University Graduate School of Medicine, Matsumoto, Nagano, Japan.
[2]Division of Gastroenterology, Department of Internal Medicine, Shinshu University School of Medicine, Matsumoto, Nagano, Japan.
[3]Department of Infectious Diseases, Internal Medicine, Graduate School of Medicine, University of Tokyo, Tokyo, Japan.
[4]Laboratory of Metabolism, National Cancer Institute, NIH, Bethesda, Maryland, USA.

Transgenic mice expressing HCV core protein develop hepatic steatosis and hepatocellular carcinoma (HCC), but the mechanism underlying this process remains unclear. Because PPARα is a central regulator of triglyceride homeostasis and mediates hepatocarcinogenesis in rodents, we determined whether PPARα contributes to HCV core protein–induced diseases. We generated PPARα-homozygous, -heterozygous, and -null mice with liver-specific transgenic expression of the core protein gene (*Ppara*$^{+/+}$:HCVcpTg, *Ppara*$^{+/-}$:HCVcpTg, and *Ppara*$^{-/-}$:HCVcpTg mice. Severe steatosis was unexpectedly observed only in *Ppara*$^{+/+}$:HCVcpTg mice, which resulted from enhanced fatty acid uptake and decreased mitochondrial β-oxidation due to breakdown of mitochondrial outer membranes. Interestingly, HCC developed in approximately 35% of 24-month-old *Ppara*$^{+/+}$:HCVcpTg mice, but tumors were not observed in the other genotypes. These phenomena were found to be closely associated with sustained PPARα activation. In *Ppara*$^{+/-}$:HCVcpTg mice, PPARα activation and the related changes did not occur despite the presence of a functional *Ppara* allele. However, long-term treatment of these mice with clofibrate, a PPARα activator, induced HCC with mitochondrial abnormalities and hepatic steatosis. Thus, our results indicate that persistent activation of PPARα is essential for the pathogenesis of hepatic steatosis and HCC induced by HCV infection.

Introduction

HCV is one of the major causes of chronic hepatitis, whereas patients with persistent HCV infection have a high incidence of hepatocellular carcinoma (HCC) (1, 2). Occurrence of HCC associated with chronic HCV infection has increased over the past 2 decades (3–5), and chronic HCV infection is recognized as a serious debilitating disease. However, the mechanism in which chronic HCV infection mediates hepatocarcinogenesis remains unclear.

HCV core protein was shown to have oncogenic potential (6). To examine how HCV core protein participates in HCV-related hepatocarcinogenesis, transgenic mouse lines were established in which HCV core protein is expressed constitutively in liver at cellular levels similar to those found in chronic HCV-infected patients (7). These mice exhibited hepatic steatosis (7) and insulin resistance (8) as early as 3 months of age; on further aging, these symptoms worsened and hepatic adenomas developed in approximately 30% of mice between 16 and 18 months of age (9). Finally, HCC was found within hepatic adenomas in a classic "nodule-in-nodule" pathology (9). Interestingly, no hepatic inflammation or fibrosis was found in these mice throughout the course of HCC development (9), which suggested that the HCV core protein itself induces hepatic steatosis and HCC independently of hepatitis.

Several studies support the contention that hepatic steatosis promotes the development of HCC (10). Epidemiologic data have identified hepatic steatosis as a major accelerating factor of hepatocarcinogenesis in chronic HCV-infected patients (11). Moreover, increases in ROS production that can cause oxidative DNA damage, mitochondrial abnormalities, and accelerated hepatocyte proliferation were observed in the steatotic livers (12–14). Thus, an intriguing possibility has emerged that alteration of fatty acid metabolism in hepatocytes may be central to the pathogenesis of HCC induced by HCV core protein.

PPARs are ligand-activated nuclear receptors belonging to the steroid/thyroid hormone receptor superfamily; 3 isoforms designated as α, β/δ, and γ exist, all of which are involved in lipid homeostasis (15). PPARα regulates constitutive transcription of genes encoding fatty acid–metabolizing enzymes (16) and is associated with the maintenance of fatty acid transport and metabolism, primarily in liver, kidney, and heart. Administration of PPARα agonists, such as the widely prescribed fibrate drugs clofibrate, gemfibrozil, and fenofibrate, ameliorate hyperlipidemia in humans (17) and hepatic steatosis in mice (18).

On the other hand, long-term administration of PPARα ligands to rodents causes accelerated hepatocyte proliferation, increased ROS generation, and development of HCC (19, 20). Disruption of the PPARα gene was shown to prevent the development of HCC caused by long-term exposure to PPARα activators (21). Interestingly, accumulation of fatty acids/triglycerides in hepatocytes

Nonstandard abbreviations used: ACC, acetyl-CoA carboxylase; AOX, acyl-CoA oxidase; CDK, cyclin-dependent kinase; CYP4A1, cytochrome P450 4A1; FAS, fatty acid synthase; FAT, fatty acid translocase; FATP, fatty acid transport protein; HCC, hepatocellular carcinoma; HCVcpTg, HCV core protein–expressing transgenic; L-FABP, liver fatty acid-binding protein; MCAD, medium-chain acyl-CoA dehydrogenase; MTP, microsomal transfer protein; 8-OHdG, 8-hydroxy-2′-deoxyguanosine; PCNA, proliferating cell nuclear antigen; RXRα, retinoid X receptor α.

Conflict of interest: The authors have declared that no conflict of interest exists.

Citation for this article: *J. Clin. Invest.* **118**:683–694 (2008). doi:10.1172/JCI33594.

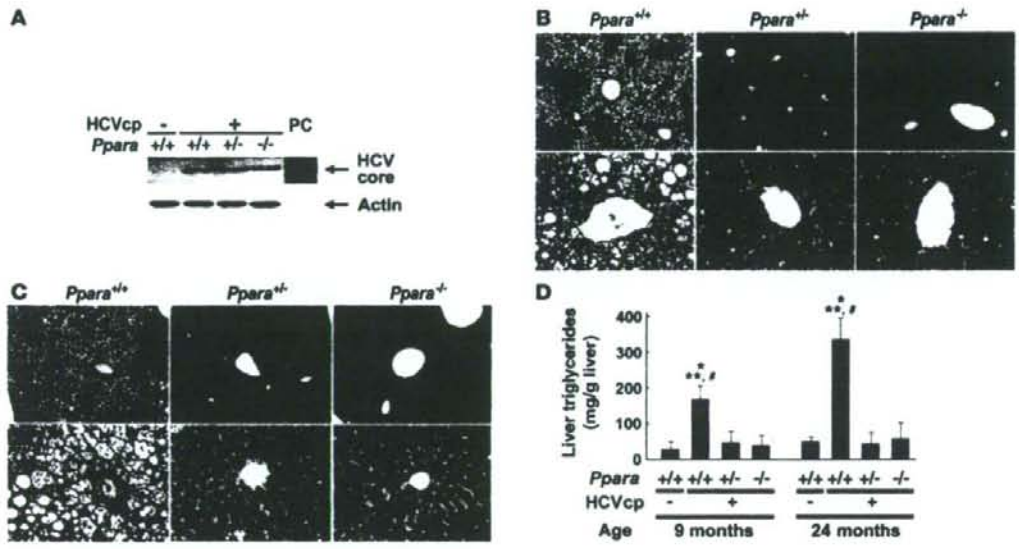

Figure 1

Phenotype changes in transgenic mouse liver. (**A**) Immunoblot analysis of HCV core protein expression in livers of 9-month-old mice. Because no significant individual differences in the same mouse group were found in the preliminary experiments, 10 mg of liver prepared from each mouse ($n = 6$ /group) was mixed and homogenized. Whole-liver lysate (50 μg protein) was loaded in each well. The band of actin was used as the loading control. Results are representative of 4 independent experiments. PC, lysate prepared from COS-1 cells overexpressing HCV core protein as a positive control. (**B**) Histological appearance of hematoxylin- and eosin-stained liver sections from 9-month-old HCVcpTg mice. Upper and lower rows show a lower (×40) and higher (×400) magnification, respectively. Microvesicular and macrovesicular steatosis was found only in *Ppara*$^{+/+}$:HCVcpTg mice. No inflammation or hepatocyte degeneration was evident in any of the genotypes. (**C**) Histological appearance of hematoxylin- and eosin-stained liver sections from 24-month-old HCVcpTg mice. Upper and lower rows show a lower (×40) and higher (×400) magnification, respectively. Hepatic steatosis was marked in *Ppara*$^{+/+}$:HCVcpTg mice, but not in other mice. Hepatic inflammation, fibrosis, and hepatocyte degeneration were not observed. In *Ppara*$^{+/-}$:HCVcpTg and *Ppara*$^{-/-}$:HCVcpTg mice, dysplastic hepatocytes and precancerous lesions were not detected throughout the entire liver. (**D**) Content of liver triglycerides. Results are expressed as the mean ± SD ($n = 6$/group) and compared between genotypes at the same age. $^{*}P < 0.05$ compared with *Ppara*$^{+/+}$ nontransgenic mice; $^{**}P < 0.05$ compared with *Ppara*$^{+/-}$:HCVcpTg mice; $^{\#}P < 0.05$ compared with *Ppara*$^{-/-}$:HCVcpTg mice.

could lead to continuous PPARα activation because of the presence of fatty acid metabolites that serve as natural PPARα ligands. For example, mice lacking expression of the peroxisomal acyl-CoA oxidase (AOX) gene showed massive accumulation of very-long-chain fatty acids in hepatocytes, severe microvesicular steatosis, chronic PPARα activation, and development of hepatic adenoma and HCC by 15 months of age (22). These results suggest a strong contribution of activated PPARα to liver tumorigenesis.

On the basis of several lines of evidence, we hypothesized that PPARα might contribute to hepatocarcinogenesis in HCV core protein–expressing transgenic (HCVcpTg) mice. To explore this possibility, PPARα-homozygous (*Ppara*$^{+/+}$), PPARα-heterozygous (*Ppara*$^{+/-}$), and PPARα-null (*Ppara*$^{-/-}$) mice bearing the HCV core protein gene, designated *Ppara*$^{+/+}$:HCVcpTg, *Ppara*$^{+/-}$:HCVcpTg, and *Ppara*$^{-/-}$:HCVcpTg mice, were generated, and phenotypic changes were examined. Surprisingly, we found that severe hepatic steatosis and HCC induced by HCV core protein developed only in *Ppara*$^{+/+}$ mice, which were related to persistent PPARα activation.

Results

Expression of HCV core protein in transgenic mice. *Ppara*$^{-/-}$:HCVcpTg and *Ppara*$^{+/-}$:HCVcpTg mice appeared healthy, and body weight in both genotypes was similar to that of *Ppara*$^{+/+}$:HCVcpTg and *Ppara*$^{+/+}$ mice without the transgene. When hepatic expression of HCV core protein in 9-month-old transgenic mice was examined by immunoblot analysis, it was similar among *Ppara*$^{+/+}$:HCVcpTg, *Ppara*$^{+/-}$:HCVcpTg, and *Ppara*$^{-/-}$:HCVcpTg mice (Figure 1A) and was also similar to expression in HCVcpTg mice reported previously (7, 9). Age and sex had only a minor influence on the hepatic expression of HCV core protein.

Requirement of homozygous PPARα for the development of hepatic steatosis in transgenic mice. Livers of 9-month-old male HCVcpTg mice with or without the *Ppara* allele were examined. Those of *Ppara*$^{+/+}$:HCVcpTg mice were soft, slightly enlarged, and light in color and histologically showed macrovesicular and microvesicular steatosis with no apparent inflammation or hepatocyte necrosis (Figure 1B), in agreement with previous reports (7, 9). Biochemical analysis of liver extracts showed marked hepatic accumulation of triglycerides (Figure 1D). In contrast, livers of 9-month-old *Ppara*$^{+/-}$:HCVcpTg and *Ppara*$^{-/-}$:HCVcpTg mice showed neither histological abnormalities nor accumulation of triglycerides (Figure 1, B and D). Hepatic levels of free fatty acids in *Ppara*$^{+/+}$:HCVcpTg mice were approximately 3 times those in *Ppara*$^{+/-}$:HCVcpTg and *Ppara*$^{-/-}$:HCVcpTg mice or *Ppara*$^{+/+}$ mice not expressing the HCV core protein.

In 24-month-old *Ppara*$^{+/+}$:HCVcpTg mice, hepatic steatosis was found (Figure 1C), and the hepatic levels of triglycerides were further increased (Figure 1D). Apparent inflammation, hepatocyte